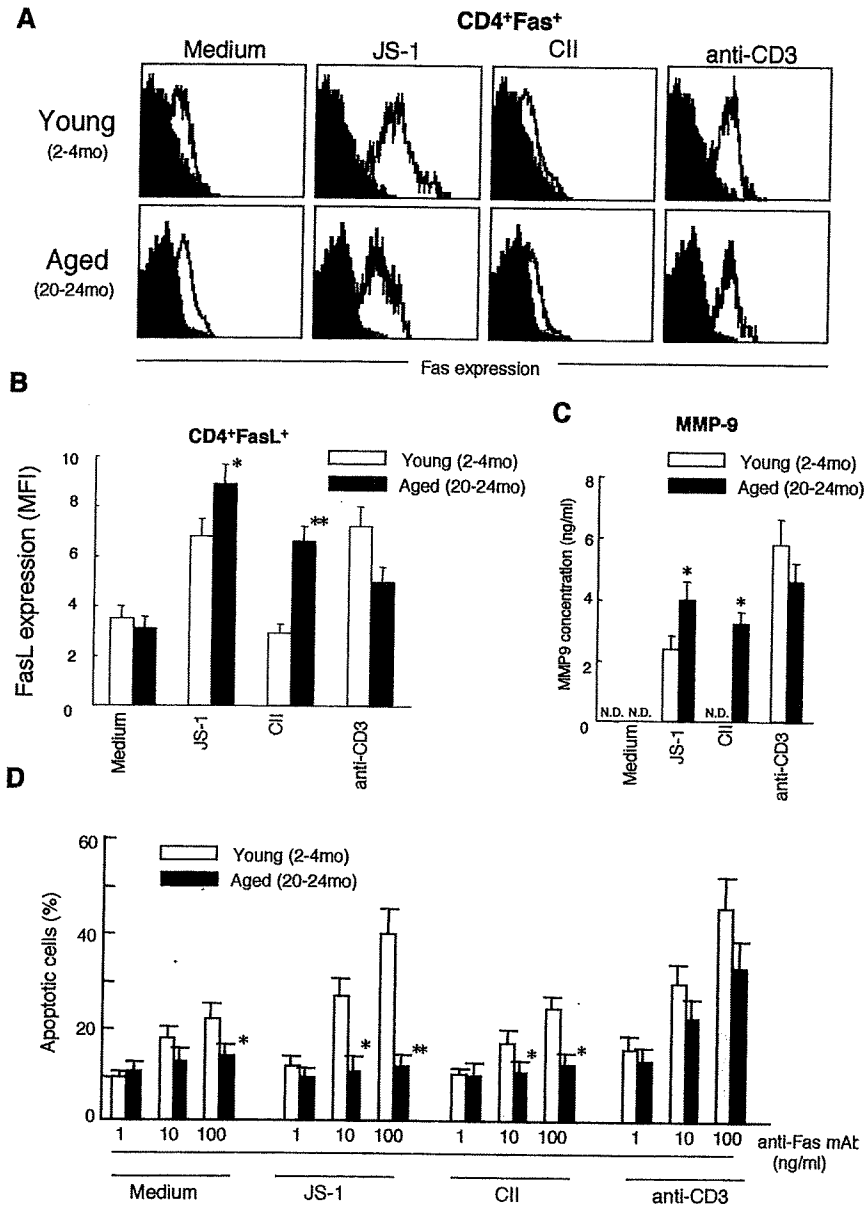

Figure 5. Expression of Fas, Fas ligand (FasL), and matrix metalloproteinase 9 (MMP-9). **A,** As shown by flow cytometry, an increased number of CD4+,Fas+ T cells was observed in JS-1–stimulated spleens from young SS model mice, but not from aged SS model mice. No significant difference was found in the numbers of CD4+,Fas+ T cells in CII-stimulated spleens from young versus aged SS model mice. **B,** A large proportion of CD4+ T cells expressing FasL was observed in spleens from aged SS model mice stimulated with either JS-1 or CII, but not in spleens stimulated with anti-CD3 monoclonal antibodies (mAb). Values are the mean and SD. * = $P < 0.05$; ** = $P < 0.01$, by Student's *t*-test. **C,** By enzyme-linked immunosorbent assay, an increased concentration of MMP-9 was detected in culture supernatant from JS-1– and CII-stimulated splenic T cells from aged SS model mice, but not in culture supernatant from anti-CD3 mAb–stimulated splenic T cells from young SS model mice. Values are the mean and SD. * = $P < 0.05$ by Student's *t*-test. **D,** Stimulation with autoantigens (JS-1 and CII) resulted in a significant, dose-dependent decrease in anti-Fas–induced CD4+ T cell apoptosis. Values are the mean and SD. * = $P < 0.05$; ** = $P < 0.01$, by Student's *t*-test. MFI = mean fluorescence intensity; ND = not detected (see Figure 3 for other definitions).

proliferation with advancing age (Figure 4C). In contrast, impaired proliferative responses were observed with advancing age upon stimulation with anti-CD3 and lipopolysaccharide. These data suggest that α-fodrin–reactive T cells may proliferate against a different antigenic epitope, which is followed by bystander T cell

activation, resulting in the development of autoimmune lesions in aged SS model mice.

Expression of Fas, FasL, and MMP-9. We next analyzed the numbers of Fas- and FasL-expressing splenic CD4+ T cells from young (ages 2–4 months) and aged (ages 20–24 months) SS model mice. An increased number of CD4+,Fas+ T cells was observed in spleens from young SS model mice, but not from aged SS model mice, stimulated with JS-1 (Figure 5A). No significant difference was found in the numbers of CD4+,Fas+ T cells in CII-stimulated spleens from young versus aged SS model mice (Figure 5A). A large proportion of CD4+ T cells expressing FasL was observed in spleens from aged SS model mice stimulated with either JS-1 or CII, but not in spleens stimulated with anti-CD3 mAb (Figure 5B). We previously detected a significantly increased concentration of MMP-9 in culture supernatant from JS-1–stimulated splenic T cells activated with anti-CD3 mAb from SS model mice (32). In the present study, we detected an increased concentration of MMP-9 in culture supernatant from JS-1– and CII-stimulated splenic T cells from aged SS model mice (Figure 5C). Moreover, it was demonstrated that autoantigen (JS-1 and CII) stimulation resulted in a significant, dose-dependent decrease in anti-Fas–induced CD4+ T cell apoptosis (Figure 5D), indicating the impairment of anti-Fas–induced T cell apoptosis in aged SS model mice. These data suggest that autoantigen stimulation may participate in immune dysregulation in the periphery in aged SS model mice.

DISCUSSION

We have used the NFS/*sld* mouse model of SS to study the age-related changes in the development of extraglandular manifestations of autoimmune lesions, and we have found that severe autoimmune arthritis developed with age in 12- and 24-month-old mice. An age-related dysregulation of immune functions in the murine model of SS resulted in a significant increase in serum levels of RF, anti-ssDNA antibodies, and anti-CII antibodies, and these changes increased with age.

Fas-mediated AICD is an important mechanism of peripheral T cell tolerance (7,33,34). Mice or humans lacking functional Fas or FasL display profound lymphoproliferative reactions associated with autoimmune disorders (35,36). We have previously demonstrated that Fas-mediated AICD is down-regulated by JS-1 autoantigen stimulation in spleen cells from SS model mice (32). In proteoglycan-induced arthritis, CD4+ T cells proliferate at a high rate in response to proteoglycan stimulation (37) and exhibit a Th1-type response (38). These observations suggest that a defect in AICD of autoreactive Th1 cells may contribute to the pathogenesis of the disease.

Our data demonstrated that splenic T cells from SS model mice contained higher levels of IL-2 and IFNγ with advancing age, and that a high titer of serum autoantibodies against α-fodrin autoantigen fragments (containing different epitopes that were originally identified in primary SS model mice) was frequently detected in young and aged SS model mice. We detected significantly increased proliferation in spleen cells from aged SS model mice stimulated with 2.7A and 3′DA protein. Our data suggest that α-fodrin autoantigen induces Th1 immune responses and accelerates disturbance of the Fas-mediated T cell apoptosis pathway in aged SS model mice.

We further observed that the spleen cells in aged SS model mice showed a significant increase in CII-specific T cell proliferation, which increased with age. CII, the main constituent of hyaline cartilage, has been proposed as one possible candidate autoantigen in rheumatoid arthritis (RA), because CII-specific antibodies are frequently found in RA patients and because an RA-like disease can be induced in certain mouse strains after immunization with CII. Our data showed a significant increase in production of serum autoantibodies against different fragments of α-fodrin autoantigen and against CII with aging, by ELISA. Moreover, significant proliferative responses against 2 α-fodrin fragments (2.7A and 3′DA) were observed in spleen cells from aged SS model mice, suggesting that bystander T cell activation may play an important role in the development of autoimmune lesions in these mice. It is possible that down-regulation of Fas-mediated AICD plays a major role in the accelerated development of autoimmune lesions with aging in the murine model of SS.

Epitope spreading has been generally proposed to contribute to the chronic pathogenesis of T cell–mediated autoimmune diseases, including experimental autoimmune encephalomyelitis (EAE) (39,40) and spontaneous diabetes in the nonobese diabetic mouse (41,42). However, it remains unclear whether T cells specific for endogenous epitopes play a significant pathologic role in tissue damage during the clinical episodes. CD4+ T cells are susceptible to AICD induced through T cell receptor (TCR)–mediated recognition of allogeneic class II MHC molecules (43,44). Our data demonstrate that autoantigen (JS-1 and CII) stimulation results in a significant, dose-dependent decrease in anti-Fas–induced CD4+ T cell apoptosis. In addition,

AICD is triggered in CD4+ T cells by the specific antigenic peptide (e.g., tetanus toxoid or myelin basic protein) presented by the appropriate class II MHC molecules (45), supporting the notion that AICD can be triggered in activated cells through the TCR-mediated recognition of antigen. Autoimmune epitope spreading has been described in patients with systemic lupus erythematosus, multiple sclerosis, and bullous pemphigus (46,47), and it is reported to be B7-1 dependent, playing a major pathologic role in EAE in mice (48). By the time a patient is diagnosed as having an autoimmune disease, significant tissue destruction has already occurred, making it difficult to identify the antigen against which the autoimmune response is directed (47).

It has been shown that membrane FasL is cleaved into a 26-kd soluble form by an MMP (49,50). We previously detected a 26-kd soluble form of FasL and MMP-9 exclusively in JS-1–stimulated splenic T cells in SS model mice (32). In the present study, we detected a significantly increased concentration of MMP-9 in culture supernatant from JS-1– and CII-stimulated splenic T cells activated with anti-CD3 mAb from aged SS model mice. It is possible that autoantigen (JS-1 and/or CII)–stimulated MMP-9 production may play an important role in down-regulation of Fas-mediated AICD, and in bystander T cell activation, resulting in accelerated development of autoimmune lesions.

In conclusion, these results suggest that age-related disturbance of AICD may play a major role in accelerated development of autoimmune lesions. The functional assays of cellular autoimmunity provide convincing evidence for impaired T cell tolerance to a set of closely related self determinants.

REFERENCES

1. Miller RA. The aging immune system: primers and prospectus. Science 1996;273:70–4.
2. Pawelec G, Adibadeh M, Pohla H, Schaudt K. Immunosenescence: ageing of the immune system. Immunol Today 1995;16: 420–2.
3. Kiecolt-Glaser JK, Preacher KJ, MacCallum RC, Atkinson C, Malarkey WB, Glaser R. Chronic stress and age-related increases in the proinflammatory cytokine IL-6. Proc Natl Acad Sci U S A 2003;100:9090–5.
4. Straub RH, Scholmerich J, Cutolo M. The multiple facets of premature aging in rheumatoid arthritis. Arthritis Rheum 2003: 48:2713–21.
5. Bardos T, Zhang J, Mikecz K, David CS, Glant TT. Mice lacking endogenous major histocompatibility complex class II develop arthritis resembling psoriatic arthritis at an advanced age. Arthritis Rheum 2002;46:2465–75.
6. Brunner T, Mogil RJ, LaFace D, Yoo NJ, Mahboubi A, Echeverri F, et al. Cell-autonomous Fas(CD95)/Fas-ligand interaction mediates activation-induced apoptosis in T-cell hybridomas. Nature 1995;373:441–4.
7. Ju ST, Panka DJ, Cui H, Ettinger R, el-Khatib M, Sherr DH, et al. Fas(CD95)/FasL interactions required for programmed cell death after T-cell activation. Nature 1995;373:444–8.
8. Hodes RJ. Molecular alterations in the aging immune system. J Exp Med 1995;182:1–3.
9. Nagel JE, Chopra RK, Chrest FJ, McCoy MT, Schneider EL, Holbrook NJ, et al. Decreased proliferation, interleukin 2 synthesis, and interleukin 2 receptor expression are accompanied by decreased mRNA expression in phytohemagglutinin-stimulated cells from elderly donors. J Clin Invest 1988;81:1096–102.
10. Proust JJ, Filburn CR, Harrison SA, Buchholz MA, Nordin AA. Age-related defect in signal transduction during lectin activation of murine T lymphocytes. J Immunol 1988;139:1472–8.
11. Critchfield JM, Racke MK, Zuniga-Pflucker JC, Cannella B, Raine CS, Goverman J, et al. T cell deletion in high antigen dose therapy of autoimmune encephalomyelitis. Science 1994;263: 1139–43.
12. Chen Y, Inobe JI, Marks R, Gonnella P, Kuchroo VK, Weiner HL. Peripheral deletion of antigen-reactive T cells in oral tolerance. Nature 1995;376:177–80.
13. Thompson CB. Apoptosis in the pathogenesis and treatment of disease. Science 1995;267:1456–62.
14. Webb S, Morris C, Sprent J. Extrathymic tolerance of mature T cells: clonal elimination as a consequence of immunity. Cell 1990;63:1249–56.
15. Nagata S, Suda T. Fas and Fas ligand: lpr and gld mutations. Immunol Today 1995;16:39–43.
16. Van Parijs L, Ibraghimov LA, Abbas AK. The roles of costimulation and Fas in T cell apoptosis and peripheral tolerance. Immunity 1996;4:321–8.
17. Drappa J, Brot N, Elkon KB. The Fas protein is expressed at high levels on $CD4^+CD8^+$ thymocytes and activated mature lymphocytes in normal mice but not in the lupus-prone strain, MRLlpr/lpr. Proc Natl Acad Sci U S A 1993;90:10340–4.
18. Fox RI, Stern M, Michelson P. Update in Sjogren's syndrome. Curr Opin Rheumatol 2000;12:391–8.
19. Manoussakis MN, Moutsopoulos HM. Sjogren's syndrome: current concepts. Adv Intern Med 2001;47:191–217.
20. Talal N, Sokoloff L, Barth WF. Extrasalivary lymphoid abnormalities in Sjogren's syndrome. Am J Med 1967;43:50–65.
21. James JA, Gross T, Scofield RH, Harley JB. Immunoglobulin epitope spreading and autoimmune disease after peptide immunization: Sm B/B9-derived PPPGMRPP and PPPGIRGP induce spliceosome autoimmunity. J Exp Med 1995;181:453–61.
22. McRae BL, Vanderlugt CL, dal Canto MC, Miller SD. Functional evidence for epitope spreading in the relapsing pathology of experimental autoimmune encephalomyelitis. J Exp Med 1995; 182:75–85.
23. Yu M, Johnson JM, Tuohy VK. A predictable sequential determinant spreading cascade invariably accompanies progression of experimental autoimmune encephalomyelitis: a basis for peptide-specific therapy after onset of clinical disease. J Exp Med 1996; 183:1777–88.
24. Zhao ML, Fritz RB. The immune response to a subdominant epitope in myelin basic protein exon-2 results in immunity to intra- and intermolecular dominant epitopes. J Neuroimmunol 1995;61: 179–84.
25. Tian J, Atkinson MA, Clare-Salzler M, Herschenfeld A, Forsthuber T, Lehmann PV, et al. Nasal administration of glutamate decarboxylase (GAD65) peptides induces Th2 responses and prevents murine insulin-dependent diabetes. J Exp Med 1996;183: 1561–7.
26. Haneji N, Hamano H, Yanagi K, Hayashi Y. A new animal model for primary Sjogren's syndrome in NFS/sld mutant mice. J Immunol 1994;153:2769–77.

27. Edwards CK III, Zhou T, Zhang J, Baker TJ, De M, Long RE, et al. Inhibition of superantigen-induced proinflammatory cytokine production and inflammatory arthritis in MRL-lpr/lpr mice by a transcriptional inhibitor of TNF-α. J Immunol 1996;157:1758–72.
28. Haneji N, Nakamura T, Takio K, Yanagi K, Higashiyama H, Saito I, et al. Identification of α-fodrin as a candidate autoantigen in primary Sjogren's syndrome. Science 1997;276:604–7.
29. Feeney AJ, Lawson BR, Kono DH, Theofilopoulos AN. Terminal deoxynucleotidyl transferase deficiency decreases autoimmune disease in MRL-Fas^{lpr} mice. J Immunol 2001;167:3486–93.
30. Fields ML, Sokol CL, Eaton-Bassiri A, Seo S, Madaio MP, Erikson J. Fas/fas ligand deficiency results in altered localization of anti-double-stranded DNA B cells and dendritic cells. J Immunol 2001;167:2370–8.
31. Kageyama Y, Koide Y, Yoshida A, Uchijima M, Arai T, Miyamoto S, et al. Reduced susceptibility to collagen-induced arthritis in mice deficient in IFN-γ receptor. J Immunol 1998;161:1542–8.
32. Ishimaru N, Yanagi K, Ogawa K, Suda T, Saito I, Hayashi Y. Possible role of organ-specific autoantigen for activation-induced cell death (AICD) in murine Sjogren's syndrome. J Immunol 2001;167:6031–7.
33. Alderson MR, Tough TW, Davis-Smith T, Braddy S, Falk B, Schooley KA, et al. Fas ligand mediates activation-induced cell death in human T lymphocytes. J Exp Med 1995;181:71–7.
34. Dhein J, Walczak H, Baumler C, Debatin KM, Krammer PH. Autocrine T-cell suicide mediated by APO-1/(Fas/CD95). Nature 1995;373:438–41.
35. Rieux-Laucat F, le Deist F, Hivroz C, Roberts AG, Debatin KM, Fischer A, et al. Mutations in Fas associated with human lymphoproliferative syndrome and autoimmunity. Science 1995;268:1347–9.
36. Fisher GH, Rosenberg FJ, Strauss SE, Dale JK, Middleton LA, Lin AY, et al. Dominant interfering Fas gene mutations impair apoptosis in a human autoimmune lymphoproliferative syndrome. Cell 1995;81:935–46.
37. Buzas EI, Mikecz K, Brennan FR, Glant TT. Mediators of autopathogenic effector cells in proteoglycan-induced arthritic and clinically asymptomatic BALB/c mice. Cell Immunol 1994;158:292–304.
38. Finnegan A, Mikecz K, Tao P, Glant TT. Proteoglycan (aggrecan)-induced arthritis in BALB/c mice is a Th1-type disease regulated by Th2 cytokines. J Immunol 1999;163:5383–90.
39. Lehmann PV, Forsthuber T, Miller A, Sercarz EE. Spreading of T-cell autoimmunity to cryptic determinants of an autoantigen. Nature 1992;358:155–7.
40. Tan LJ, Kennedy MK, dal Canto MC, Miller SD. Successful treatment of paralytic relapses in adoptive experimental autoimmune encephalomyelitis via neuroantigen-specific tolerance. J Immunol 1991;147:1797–802.
41. Kaufman DL, Clare-Salzler M, Tian J, Forsthuber T, Ting GS, Robinson P, et al. Spontaneous loss of T cell tolerance to glutamic acid decarboxylase in murine insulin-dependent diabetes. Nature 1993;366:69–71.
42. Tisch R, Yang XD, Singer SM, Liblau RS, Fugger L, McDevitt HO. Immune response to glutamic acid decarboxylase correlates with insulitis in non-obese diabetic mice. Nature 1993;366:72–5.
43. Kabelitz D, Oberg HH, Pohl T, Pechhold K. Antigen-induced death of mature T lymphocytes: analysis by flow cytometry. Immunol Rev 1994;142:157–74.
44. Damle NK, Klussman K, Leytze G, Aruffo A, Linsley PS, Ledbetter JA. Costimulation with integrin ligands intercellular adhesion molecule-1 or vascular cell adhesion molecule-1 augments activation-induced death of antigen-specific CD4$^+$ T lymphocytes. J Immunol 1993;151:2368–79.
45. Pelfrey CM, Tranquill LR, Boehme SA, McFarland HF, Lenardo MJ. Two mechanisms of antigen-specific apoptosis of myelin basic protein (MBP)-specific T lymphocytes derived from multiple sclerosis patients and normal individuals. J Immunol 1995;154:6191–202.
46. Vanderlugt CL, Neville KL, Nikcevich KM, Eagar TN, Bluestone JA, Miller SD. Pathologic role and temporal appearance of newly emerging autoepitopes in relapsing experimental autoimmune encephalomyelitis. J Immunol 2000;164:670–8.
47. Perriard J, Jaunin F, Favre B, Budinger L, Hertl M, Saurat JH, et al. IgG autoantibodies from bullous pemphigoid (BP) patients bind antigenic sites on both the extracellular and the intracellular domains of the BP antigen 180. J Invest Dermatol 1999;112:141–7.
48. Grenet J, Teitz T, Wei T, Valentine V, Kidd VJ. Structure and chromosome localization of the human CASP8 gene. Gene 1999;226:225–32.
49. Kayagaki N, Kawasaki A, Ebata T, Ohmoto H, Ikeda S, Inoue S, et al. Metalloproteinase-mediated release of human Fas ligand. J Exp Med 1995;182:1777–83.
50. Gearing AJ, Beckett P, Christodoulou M, Churchill M, Clements J, Davidson AH, et al. Processing of tumor necrosis factor-α precursor by metalloproteinases. Nature 1994;370:555–7.

American Journal of Pathology, Vol. 165, No. 1, July 2004

Molecular Analysis of the Human Autoantibody Response to α-Fodrin in Sjögren's Syndrome Reveals Novel Apoptosis-Induced Specificity

Toshiaki Maruyama,* Ichiro Saito,† Yoshio Hayashi,‡ Elizabeth Kompfner,* Robert I. Fox,§ Dennis R. Burton,* and Henrik J. Ditzel*¶‖

From the Department of Immunology, The Scripps Research Institute, La Jolla, California; the Allergy and Rheumatology Clinic,§ The Scripps Memorial Hospital, La Jolla, California; the Department of Pathology,† Tsurumi University School of Dental Medicine, Yokohama, Japan; the Department of Pathology,‡ Tokushima University School of Dentistry, Tokushima, Japan; Center of Medical Biotechnology,¶ Institute of Medical Biology, University of Southern Denmark, Odense, Denmark; and Department of Internal Medicine C,‖ Odense University Hospital, Odense, Denmark*

Lymphocyte infiltration of salivary and lacrimal glands leading to diminished secretion and gland destruction as a result of apoptosis is thought to be pivotal in the pathogenesis of Sjögren's syndrome (SS). The cytoskeletal protein α-fodrin is cleaved during this apoptotic process, and a strong antibody (Ab) response is elicited to a 120-kd fragment of cleaved α-fodrin in the majority of SS patients, but generally not in other diseases in which apoptosis also occurs. Little is known about the anti-α-fodrin autoantibody response on a molecular level. To address this issue, IgG phage display libraries were generated from the bone marrow of two SS donors and a panel of anti-α-fodrin IgGs was isolated by selection on α-fodrin immunoblots. All of the human monoclonal Abs (hmAbs) reacted with a 150-kd fragment and not with the 120-kd fragment or intact α-fodrin, indicating that the epitope recognized became exposed after α-fodrin cleavage. Analysis of a large panel of SS patients (defined by the strict San Diego diagnostic criteria) showed that 25% of SS sera exhibited this 150-kd α-fodrin specificity. The hmAbs stained human cultured salivary acinar cells and the staining was redistributed to surface blebs during apoptosis. They also stained inflamed acinar/ductal epithelial cells in SS salivary tissue biopsies, and only partially co-localized with monoclonal Abs recognizing the full-length α-fodrin. Our study shows that in SS patients, neoepitopes on the 150-kd cleaved product of α-fodrin become exposed to the immune system, frequently eliciting anti-150-kd α-fodrin Abs in addition to the previously reported anti-120-kd Abs. The anti-150-kd α-fodrin hmAbs may serve as valuable reagents for the study of SS pathogenesis and diagnostic analyses of SS salivary gland tissue. ***(Am J Pathol 2004, 165:53–61)***

Sjögren's syndrome (SS) is the second most common autoimmune rheumatic disease, causing ocular and oral dryness and extraglandular manifestations in three to four million people in the United States alone.[1–3] The disease is characterized by lymphocytic infiltrates and destruction of the salivary and lacrimal glands, and systemic production of characteristic autoantibodies. Xerostomia and keratojunctivitis sicca are the common clinical signs, but the San Diego SS diagnostic criteria also require a positive salivary gland biopsy or the presence of autoantibodies to the ribonucleoprotein SS-A/Ro for diagnosis;[4] these requirements are not included in the European Economic Committee diagnostic criteria.[5,6] The typical histopathological findings of SS salivary and lacrimal gland tissues include glandular attrition in acinar and ductal epithelia concomitant with lymphoplasmacytic infiltration consisting of predominantly $CD4^+$ cells, but also $CD8^+$, B cells, and plasma cells. Several immune and inflammatory effector pathways seem to be implicated in the ongoing pathology of SS, but our understanding of the initiation factors and the precise mechanism of epithelial cell damage and dysfunction remains limited.

Recent studies have indicated a 120-kd fragment of α-fodrin as a potential important autoantigen in the pathogenesis of primary SS in both a mouse model and in humans.[7–11] Fodrin is an abundant component of the membrane cytoskeleton of most eukaryotic cells. It is composed of heterodimers of an α (240 kd) and a β (235 kd) subunit that share homologous internal spectrin repeats, but have distinct amino- and carboxyl-terminal regions. The α-fodrin subunit is an actin-binding protein that may be involved in secretion[12–14] and has been shown in apoptotic cells to be cleaved by calpain,

Supported in part by a research grant from the Sjögren's Syndrome Foundation and the National Institutes of Health (grants AI41590 and HL63651 to H.J.D.).

Accepted for publication March 4, 2004.

Address reprint requests to Henrik J. Ditzel, Center of Medical Biotechnology, University of Southern Denmark, Winsloewparken 25, 3, 5000 Odense C, Denmark. E-mail: hditzel@health.sdu.dk.

caspases, and an unidentified protease present in T-cell granule content.[15–18] Indeed, treatment of mice with caspase inhibitors prevents induction of SS.[19] Autoantibodies to the 120-kd cleavage fragment of α-fodrin have been detected in patients with primary and secondary SS but also in a few systemic lupus erythematosus (SLE) patients without SS.[7,9,20–22] Different diagnostic criteria for SS have been used in the various studies and differences in the specificity of 120-kd α-fodrin for SS have been observed, which has rendered the importance of 120-kd α-fodrin as a diagnostic marker controversial.

Here, we have further evaluated the incidence and specificity of anti-α-fodrin Ab response in American SS patients and found a correlation between anti-α-fodrin Ab and SS, but a lower prevalence of anti-120-kd α-fodrin Abs in American *versus* Japanese SS patients. We also found that ~25% of SS sera contained Abs against the 150-kd cleavage fragment of α-fodrin. To examine these Abs at a molecular level, we cloned and characterized a panel of hmAbs from SS patients using phage display technology that specifically recognized the 150-kd α-fodrin neoepitope. The anti-150-kd hmAbs were shown to detect 150-kd α-fodrin in apoptotic acinar and ductal salivary gland cells in cell culture, and in SS salivary gland tissue sections, indicating that the hmAbs may be useful diagnostic reagents in SS pathology.

Materials and Methods

Patients

Sera were obtained from 60 SS patients (42 American and 18 Japanese) who fulfilled the San Diego criteria for the diagnosis of SS;[23] 12 rheumatoid arthritis (RA) patients; 12 SLE patients, diagnosed based on American College of Rheumatology criteria; and 10 healthy individuals. Bone marrow from two Caucasian American patients with secondary SS (designated SS23 and SS30) were obtained for Ab library construction.

Western Blot Analysis

α-Fodrin was purified from mouse brain tissue using the method of Cheney and colleagues[24] yielding >95% purity. Mouse α-fodrin exhibits 94% amino acid sequence identity to human α-fodrin. Coomassie staining of mouse brain α-fodrin separated by sodium dodecyl sulfate-polyacrylamide gel electrophoresis (SDS-PAGE) on a 10% Tris-HCl gel (Bio-Rad, Hercules, CA) showed an intense band at 240 kd corresponding to intact α-fodrin, but also weaker bands at 180, 150, 120, 80, 50, and 30 kd that corresponded to cleaved α-fodrin because of low levels of constitutive apoptosis, as previously reported.[14,17,24,25] Mouse brain α-fodrin separated by SDS-PAGE was also electroblotted onto polyvinylidene difluoride membrane (Immobilon P; Millipore, Bedford, MA), the membrane was blocked with 5% nonfat dry milk (Bio-Rad) in phosphate-buffered saline (PBS), pH 7.0, for 30 minutes, and incubated with serum (diluted 1:1000 in PBS), human recombinant Fabs (1 to 20 μg/ml) or mouse anti-α-fodrin mAb AA6 (Affiniti, Exeter, UK) for 1 hour on a rotator. mAb AA6 predominantly recognizes the 240-kd intact form of α-fodrin, but also the 120- and 150-kd cleaved form of α-fodrin. The membrane was washed three times (10 minutes/wash) in PBS and bound serum Ab was detected with horseradish peroxidase-conjugated goat Fab anti-human IgG (H+L) Ab (Bio-Rad). A patient serum was used as internal control in each blotting experiment to adjust for band intensity variations between gels. The intensity of the bands was scored (1 to 5) based on quantification by densitometry. Bound human recombinant Fabs were detected with horseradish peroxidase-conjugated goat anti-human IgG $F(ab')_2$ Ab and bound mouse mAb detected with horseradish peroxidase-conjugated goat anti-mouse IgG Ab (both Jackson) diluted in blocking solution and incubated for 1 hour at room temperature. After washing for 45 minutes with PBS, membranes were rinsed briefly in MilliQ water, and bound enzyme-labeled Ab was visualized using chemiluminescent substrate (SuperSignal, WestPico; Pierce, Rockford, IL) according to the manufacturer's instructions and autoradiographic film (Eastman Kodak, Rochester, NY). All incubations were done at room temperature. As controls, all experiments were performed using the anti-Ebola virus Fab ELZ510, the anti-HIV-1 gp120 Fab b12, normal sera or by omitting the primary Ab.

Analysis of Patient Sera and Human Fabs by Enzyme-Linked Immunosorbent Assay (ELISA)

Mouse brain α-fodrin (2 μg/ml) and ovalbumin (4 μg/ml) (Pierce) were coated onto microtiter wells (Costar, Cambridge, MA) at 4°C overnight. Wells were washed with PBS; blocked with 4% nonfat dry milk in PBS for 30 minutes; and incubated with patient serum (diluted 1:100 and 1:400 in PBS), human Fabs, or mouse anti-α-fodrin mAb AA6 for 1 hour at 37°C. Wells were washed six times with PBS-0.05% Tween and bound Ab was detected with alkaline phosphatase-conjugated goat IgG anti-human IgG $F(ab')_2$ Ab or anti-mouse IgG $F(ab')_2$ Ab (both 1:500 in 1% bovine serum albumin/PBS, Pierce) and visualized with nitrophenol substrate (NPP substrate) (Sigma, St. Louis, MO) by reading absorbance at 405 nm.

RNA Isolation and Library Construction

RNA was isolated from bone marrow of two American SS patients (designated SS23 and SS30) by a guanidinium isothiocyanate method, as described previously.[26] Serum samples from each donor were drawn concomitantly. After reverse-transcription, the γ1 (Fd region) and κ and λ chains were amplified by polymerase chain reaction and phage-display libraries were constructed in the phage-display vector pComb3, as described previously.[27–29]

Ab Library Selection

Libraries were selected against α-fodrin blotted membrane. Mouse brain α-fodrin was separated by SDS-

PAGE using a 10% Tris-HCl gel and transferred to polyvinylidene difluoride membranes. After blocking with 5% nonfat dry milk/PBS for 30 minutes, the membrane was incubated with phage (10^{11} pfu) resuspended in PBS containing 1% bovine serum albumin for 2 hours at room temperature. The membrane was washed and the bound phage, enriched for those bearing antigen-binding surface Fabs, were eluted with 0.2 mol/L glycine-HCl buffer, pH 2.2, as previously described.[29–31] The eluted phages were amplified by infection of *Escherichia coli* and superinfection with M13 helper phage. The libraries were panned for four consecutive rounds with increasing washing stringency (2 × 10 minutes for first panning round and 4 × 10 minutes thereafter). Phagemid DNA, isolated after the last round of panning, was digested with *Nhe*I and *Spe*I restriction endonucleases and religated to excise the cpIII gene. The reconstructed phagemid was used to transform XL1-Blue cells (Stratagene, La Jolla, CA) to produce clones secreting soluble Fab fragments. Positive Fab clones were purified from bacterial supernatants by affinity chromatography as previously described.[32]

Nucleic Acid Sequencing

Nucleic acid sequencing was performed on a 373A or 377A automated DNA sequencer (ABI, Foster City, CA) using a *Taq* fluorescent dideoxy terminator cycle sequencing kit (ABI). Sequencing primers were as reported.[33] Comparison to reported Ig germline sequences from GenBank and EMBL was performed using the Genetic Computer Group (GCG) sequence analysis program.

Confocal Laser-Scanning Microscopy Analysis of Human Cells and Tissue Biopsies

Human salivary gland (HSG) cells were grown in minimum essential medium, Eagle's, in Earle's balanced salt solution (EMEM) medium supplemented with 10% fetal calf serum and allowed to adhere to chambered coverslips (Nunc, Kamstrup, Denmark) for 48 hours at 37°C, 5% CO_2, to form monolayers. Apoptosis of HSG cells was induced by incubating the cells with 100 ng/ml of tumor necrosis factor-α (Upstate Biotechnology, Lake Placid, NY) and 1 μg/ml of cycloheximide for 3 to 15 hours at 37°C/5% CO_2. Untreated cells or those induced to undergo apoptosis were fixed by 96% ice-cold ethanol for 5 minutes at 4°C or by 4% paraformaldehyde for 10 minutes at room temperature. Paraformaldehyde-fixed cells were washed in PBS before being permeabilized in 0.005% saponin for 10 minutes at room temperature. After washing in PBS and blocking with 5% normal goat serum for 1 hour, cells were incubated with Ab. Fresh-frozen tissue was obtained from labial biopsies of patients with active SS and healthy controls. Freshly cut 5-μm sections were dried overnight, fixed by ice-cold 96% ethanol for 5 minutes at 4°C or by acetone for 10 minutes at room temperature, and blocked with 5% normal goat serum. HSG cells and tissue sections were incubated with human Fabs (10 μg/ml in PBS), or mouse anti-α-fodrin mAb AA6 (Affiniti) for 1 hour. In some experiments apoptotic cells were stained with Annexin V-FITC (Pharmingen, La Jolla, CA) for 1 hour before fixation. The slides were washed with PBS and incubated with fluorescein isothiocyanate-labeled $(Fab')_2$ goat anti-human IgG $(Fab')_2$ Ab (Jackson), and Texas Red-labeled goat anti-mouse IgG Ab (Jackson), or propidium iodine (Sigma) for 1 hour. The slides were again washed with PBS for 5 minutes and mounted with Slow Fade in PBS/glycerol (Molecular Probes, Eugene, OR) before analysis using a Zeiss Axiovert S100 TV confocal laser-scanning microscope (Zeiss, New York, NY). All incubations were performed at room temperature unless otherwise indicated. As controls, all experiments were performed using the human Fab b12 to HIV-1 gp120 or by omitting the primary Ab. Adjacent tissue sections were hematoxylin and eosin stained or stained with anti-CD3 (DAKO, Carpinteria, CA), and anti-cytokeratin 18 (CY-90; Sigma-Aldrich) mAbs to determine the cell type present.

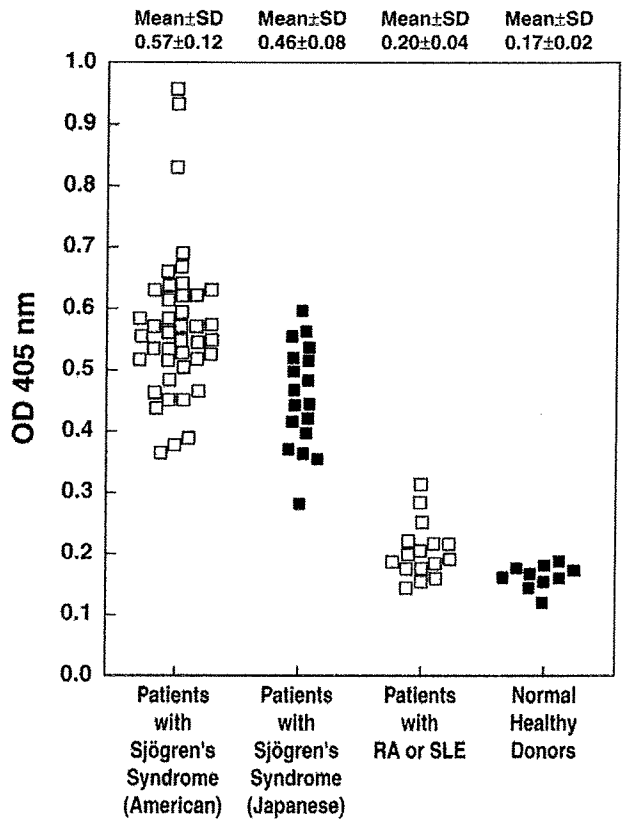

Figure 1. Sera from SS patients contain anti-α-fodrin Abs, as measured by ELISA. Sera, diluted 1:400 in PBS, from 42 American SS patients, 17 Japanese SS patients, 16 RA and SLE patients, and 10 healthy individuals were tested for binding to mouse brain α-fodrin by ELISA. Samples with A_{405} values more than twice the mean of the control normals (>0.33) were considered positive.

Results

Serological Analysis of α-Fodrin Autoantibodies in SS Patients

To investigate the specificity and sensitivity of anti-α-fodrin Abs for SS, serum from patients with SS, RA, SLE,

and healthy individuals were tested for binding to mouse brain α-fodrin by ELISA. A secondary Ab capable of detecting both IgG and IgA was used, because anti-α-fodrin Ab of both the IgG and IgA have been suggested to be elevated in SS sera. As shown in Figure 1, elevated α-fodrin Ab levels were observed in both American and Japanese SS patients compared to the RA and SLE patient groups and healthy individuals. Positivity was defined as an OD_{405} value greater than twice the mean of the normal controls (>0.33) at a serum dilution of 1:400. Sera from all of the American SS patients and all but one of the Japanese SS patients were positive for α-fodrin Abs (98%), whereas only 1 of 16 RA/SLE patients (6%), and none of the healthy donors, were positive. The mean level of anti-α-fodrin Ab in both the American (OD_{405} nm, 0.57 ± 0.12) and Japanese SS patients (OD_{405} nm, 0.46 ± 0.08) were significantly higher than healthy controls (0.17 ± 0.02, $P < 0.0001$) or the RA/SLE patients (0.20 ± 0.04, $P < 0.0001$). The mouse anti-α-fodrin mAb AA6 was included in each experiment as a control (OD_{405} nm, 0.8).

The frequency of SS sera with Abs specific for the 120-kd fragment of cleaved α-fodrin was determined by assessing binding to Western blots of mouse brain α-fodrin. Fifteen of 42 American SS sera (36%) (diluted 1:1000) exhibited reactivity against the 120-kd fragment of α-fodrin (Table 1). In addition, 10 sera showed reactivity with a 150-kd fragment of cleaved α-fodrin (24%), while 7 showed reactivity with a 180-kd fragment and other cleaved products of α-fodrin. As shown in Table 1, some patient sera reacted with multiple α-fodrin fragments, whereas the Western blot for other sera revealed reactivity with only one of the fragments. Overall, 22 American SS sera (52%) reacted with at least one form of cleaved α-fodrin. When the 17 Japanese SS sera were tested by Western blotting, the prevalence of anti-α-fodrin Ab reactivity was found to be significantly higher than in the American SS sera (12 of 17 positive, 70.6%; $P < 0.01$). All of the α-fodrin-reactive sera from the Japanese patients recognized 120-kd, but five also bound to the 150-kd α-fodrin (29.4%) (Table 1). Serum of 8 RA patients, 8 SLE patients, and 10 healthy individuals was also tested by Western blot analysis. Only one SLE serum was found to react with the 120-kd fragments of α-fodrin and none reacted with the 150-kd fragments of α-fodrin.

Table 1. Binding of American (ASSP) and Japanese (JSSP) SS Patient Sera to Cleaved Mouse Brain α-Fodrin by Western Blot Analysis

Patient	Intensity* of bands	Fragment size (kd)
ASSP1	–	
ASSP2	–	
ASSP3	1+	150
ASSP4	–	
ASSP5	–	
ASSP6	1+	120
ASSP7	3+	180
ASSP8	3+	120, 150, 50
ASSP9	2+	120
ASSP10	–	
ASSP11	–	
ASSP12	1+	150, 80, 30
ASSP13	–	
ASSP14	–	
ASSP15	–	
ASSP16	–	
ASSP17	–	
ASSP18	–	
ASSP19	1+	120, 150
ASSP20	1+	120, 150
ASSP21	–	
ASSP22	2+	150, 180
ASSP23	4+	120, 150
ASSP24	–	
ASSP25	2+	150
ASSP26	–	
ASSP27	2+	150
ASSP28	3+	120, 180
ASSP29	2+	120, 180
ASSP30	5+	150
ASSP31	3+	120
ASSP32	–	
ASSP33	–	
ASSP34	3+	120
ASSP35	2+	120, 180, 50
ASSP36	1+	120
ASSP37	–	
ASSP38	–	
ASSP39	1+	120, 180, 50
ASSP40	–	
ASSP41	2+	120, 180, 80
ASSP42	2+	120, 50
JSSP1	3+	120
JSSP2	2+	120
JSSP3	2+	120, 150
JSSP4	2+	120
JSSP5	2+	120, 150
JSSP6	1+	120
JSSP7	1+	120, 150
JSSP8	1+	120
JSSP9	1+	120
JSSP10	1+	120, 150
JSSP11	1+	120
JSSP12	1+	120, 150
JSSP13	–	
JSSP14	–	
JSSP15	–	
JSSP16	–	
JSSP17	–	

*The intensity was evaluated at a scale 1 to 5; 5 being the most intense.

Isolation of Human IgG mAbs Against the 150-kd Form of Cleaved α-Fodrin from SS Patients

To characterize the anti-150-kd α-fodrin Abs response at a molecular level, IgG_1 κ/λ Ab phage display libraries were generated from two patients (SS23 and SS30), whose sera predominantly recognized the 150-kd cleavage fragment of α-fodrin and also reacted with extract of human SS salivary gland tissue. As starting material for the Ab library construction, bone marrow was obtained from patients SS23 and SS30. Bone marrow has been shown to be a major repository for the plasma cells that produce the Abs found in the circulation. The Ab libraries from patients SS23 (≈6×10^6 members) and SS30 (≈8×10^6 members) were panned against mouse brain α-fodrin consisting of mostly intact α-fodrin, but also a small amount of apoptotic cleaved α-fodrin. The α-fodrin preparation was either separated by SDS-PAGE and

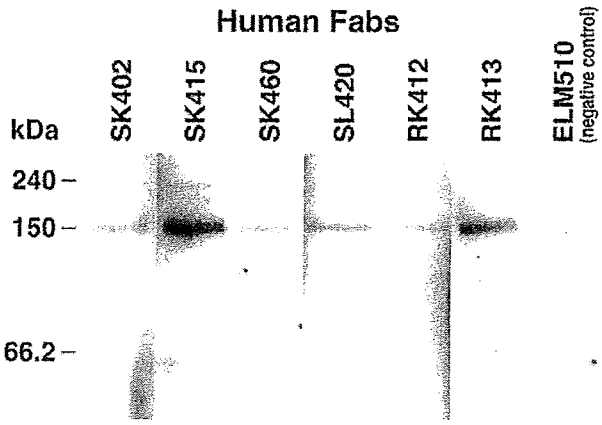

Figure 2. Binding of human monoclonal IgG Fabs to purified mouse α-fodrin brain extract by Western blot analysis. All of the Fabs specifically bound to the 150-kd fragment of cleaved α-fodrin and did not react with 240-kd intact α-fodrin. The human monoclonal anti-Ebola virus Fab ELZ510 was used as a negative control.

transferred to a polyvinylidene difluoride membrane or coated on microtiter wells. After four rounds of biopanning against α-fodrin blotted on a polyvinylidene difluoride membrane, a significant increase in eluted phage was observed, indicating enrichment for antigen-binding Fab-phages. Individual clones, expressed as soluble Fabs by excising the gene III from the pcomb3 phagemid DNA from the last round of selection, were tested for binding to α-fodrin by Western blotting. This analysis yielded 19 Fabs that exhibited strong binding to the 150-kd fragment of cleaved α-fodrin and no binding to intact α-fodrin (240 kd), although present in significant excess, or the 120-kd cleaved form of α-fodrin (Figure 2). The Fabs also failed to react with Western blots of HeLa lysate, which contained intact α-fodrin, but not 120- or 150-kd α-fodrin, as determined by staining with mouse mAb AA6. Sequencing the DNA encoding the heavy chain variable region of the 19 Fabs revealed that 4 Fabs isolated from patient SS23 (SK402, SK415, SK460, and SL420) and 2 Fabs isolated from patient SS30 (RK412 and RK413) were unique, whereas the remaining sequences were repeats of the six sequences (Table 2).

The IgG-Derived Anti-150-kd α-Fodrin Fabs Are Derived as a Result of an Affinity-Matured Antigen-Driven Antibody Response

Next, the variable heavy and light chain genes of the IgG-derived anti-150-kd α-fodrin Fab fragments were compared with the closest germline sequences in the GenBank database (Table 2). The Ab heavy chain is the major contributor to antigen-binding in many instances and so detailed analysis was focused on this chain. All of the variable heavy chain region genes of the anti-150-kd α-fodrin IgG Fabs were highly mutated, and exhibited a high replacement (R) to silent (S) mutation ratio (R/S ratio) for the complementarity determining regions (CDRs) (CDR1 and CDR2) compared to the framework regions (FR) (FR1, FR2, and FR3), characteristic of an affinity-matured antigen-driven Ab response. No particular restriction in the VH or JH gene usage of the anti-150-kd α-fodrin IgG Fabs was observed (Table 2), neither did the analysis reveal any restriction in the germline usage within the context of the VH families used. Unequivocal identification of the closest germline D segment proved impossible because of significant somatic modification.

Epitope Characterization

To pinpoint the epitopes recognized by the anti-150-kd α-fodrin human Fabs, three polypeptides spanning α-fodrin were coated on ELISA wells and tested for reactivity with the Fabs. The polypeptides included JS-1 (1 to 1784 bp), 2.7A (2258 to 4884 bp), and 3'DA (3963 to 7083 bp). None of the tested Fabs recognized any of the peptides, suggesting that the Fabs either recognized regions or partial conformational epitopes of α-fodrin not represented by the peptides.

Subcellular Distribution of 150-kd α-Fodrin in HSG Cells

To determine the subcellular distribution of the 150-kd fragment of cleaved α-fodrin, HSG cells were stained with selected human Fabs and examined by laser-scanning confocal microscopy. As shown in Figure 3, Fab SK415 and SK460 exhibited cytoplasmic staining, whereas no staining was observed with a control Fab. Similar cytoplasmic staining was also observed with mouse mAb AA6 recognizing both intact and cleaved α-fodrin (Figure 3l). As previously reported, the cytoplasmic staining of the mouse mAb AA6 was particularly intense, corresponding to the plasma membrane, but this was not observed with the human anti-150-kd α-fodrin Fabs. The fixation method of the HSG cells (ethanol or paraformaldehyde/saponin) did not seem to influence the staining patterns of Fab SK415 and mAb AA6.

Table 2. Deduced Amino Acid Sequences of the Heavy Chain CDR3 Region and Adjacent Framework Regions of Anti-150 kd, α-Fodrin IgGs

Fab	VH/germline	FR3	CDR3	FR4	JH
SK402 (3)	VH1-8	YYCAR	EGWPPTNDY	WGQ	JH4
SK415 (1)	VH3-21	YFCVR	DLCGGRDS	WGQ	JH5
SK460 (2)	VH3-33	YLCAR	EAWHDIGEYDGRRTLGSVPSLDL	WGQ	JH5
SL420 (1)	VH3-21	YYCAR	DGDGYRDY	WGQ	JH4
RK412 (8)	VH1-69	YYCAR	GFGGEDAYYDNFGYYASTEF	WGL	JH3
RK413 (4)	VH4-4	YYCAR	WGPRDLSGRSGGFDP	WGP	JH4

Number in parentheses denotes the number of Fabs that had the same heavy-chain CDR3 sequence. The closest germline gene, VH and JH families for each clone are also shown.

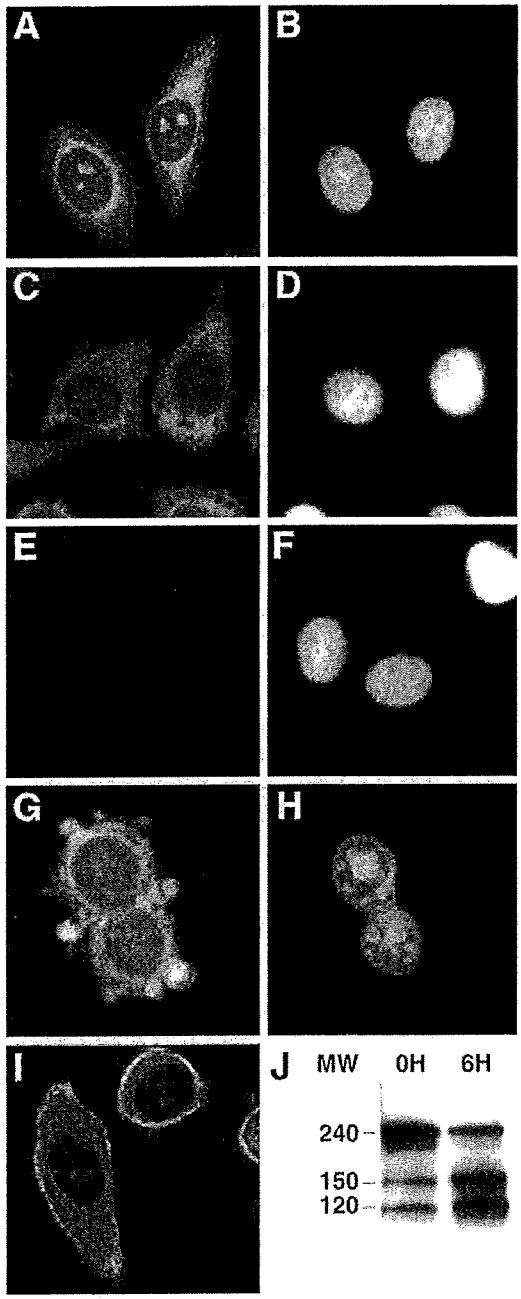

Figure 3. Subcellular distribution of intact and cleaved α-fodrin in human salivary cells. Ethanol-fixed human salivary HSG cells were stained with the human anti-150-kd α-fodrin Fabs SK415 (**A**) and SK460 (**C**), a human anti-HIV-1 gp120 Fab, b12 (**E**, negative control), and the mouse anti-α-fodrin mAb AA6 (**I**). Intense cytoplasmic staining with Fabs SK415 and SK460 and mouse mAb AA6 was observed in the permeabilized cells, although only partial co-localization between the human and mouse mAbs was observed. The cells were also stained with propidium iodine (**B**, **D**, **F**, **H**). Apoptotic HSG cells, exhibiting increased levels of cleaved 120- and 150-kd α-fodrin (**J**, 6H) compared to nonapoptotic cells (**J**, 0H), were also stained with Fab SK415 (**G**) and showed intense staining at the surface blebs.

Cleaved 150-kd α-Fodrin Is Present in Blebs of Apoptotic HSG Cells

Previous studies have shown that α-fodrin is cleaved by different apoptotic enzymes, but the question remained as to how α-fodrin, an intracellular protein, became exposed to the immune system. One possibility is that 150-kd fragments of α-fodrin are exposed on the cell surface during the morphological and biochemical process of apoptosis. Recent reports have demonstrated that certain SS-associated autoantigens, including La, translocate during apoptosis to the cell surface, and particularly to cell surface blebs.[34–36] To determine whether 150-kd α-fodrin fragments become concentrated at the surface of apoptotic HSG cells, apoptosis was induced in HSG cell cultures by tumor necrosis factor-α and cycloheximide, and the cells stained with the anti-150-kd α-fodrin Fab SK415 or anti-HIV-1 gp120 Fab (negative control), and propidium iodine (PI). Apoptotic cells were visualized by the binding of fluorescein isothiocyanate-annexin V to phosphatidylserine on the cell surface before fixation and by morphological appearance, including nuclear condensation, surface blebbing, and cell shrinkage (Figure 3, G and H). HSG cell cultures induced by tumor necrosis factor-α and cycloheximide to undergo apoptosis were also analyzed by Western blot and showed increased levels of cleaved 120- and 150-kd α-fodrin (Figure 3J, 6H) compared to noninduced HSG cell cultures, which contained only low amounts of constitutive apoptotic cells, as previously reported (Figure 3J, 0H).[14,17] Confocal analysis demonstrated that anti-150-kd α-fodrin translocated to cell surface blebs of apoptotic HSG cells (Figure 3G). No staining was observed with a control human Fab Ab against HIV-1 gp120 (data not shown).

Localization of 150-kd Cleaved α-Fodrin within SS Salivary Gland Tissue

To determine the distribution of 150-kd fragments of α-fodrin in salivary tissue from patients with active SS, fresh-frozen labial biopsies from three SS patients were obtained and examined by immunohistochemistry. Cryostat tissue sections were stained with anti-150-kd α-fodrin Fab SK415 and a mouse anti-α-fodrin mAb AA6 (Figure 4, A and B). Laser-scanning confocal microscopy of the SS-infiltrated salivary gland using SK415 revealed intense staining of the acinar epithelia cells, with intensification at the cell surface and co-localization with the mouse anti-α-fodrin mAb (Figure 4C, solid arrows). However, SK415 also exhibited intense patchy staining corresponding to the lymphocytic infiltrate immediately surrounding the affected acini, an area not stained by the mAb AA6 or the fluorescein isothiocyanate-labeled anti-human $F(ab')_2$ Ab alone (Figure 4, open arrows). The SK415 staining in this area was not confined to cells, but seemed to be associated with 150-kd α-fodrin, which had leaked from inflamed glandular cells. The unaffected duct cells were stained by mAb AA6 (Figure 4, arrowheads), but only weakly by Fab SK415. Similarly, duct cells from normal salivary gland tissue were stained by mAb AA6, but not, or only weakly, by Fab SK415 (Figure 4D). The fixation method of the labial biopsy sections (ethanol or acetone) did not seem to influence the staining patterns of Fab SK415 and mAb AA6.

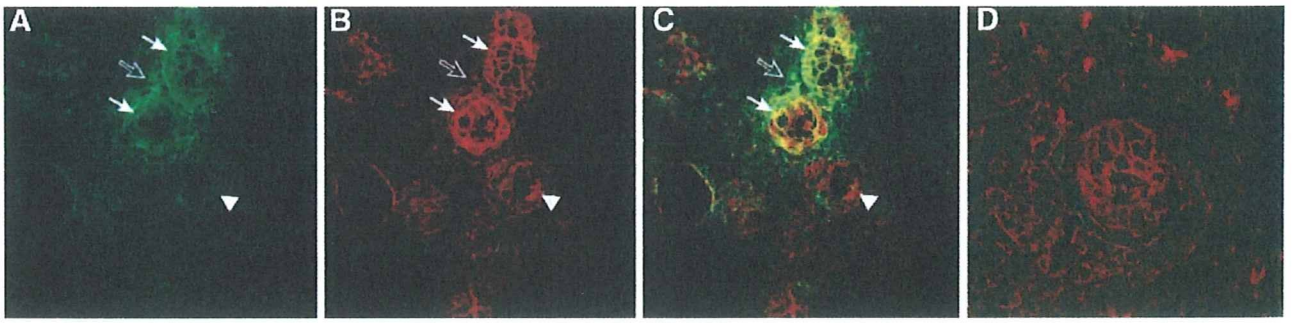

Figure 4. Distribution of cleaved and intact α-fodrin in salivary gland tissue of a SS patient with active disease. Tissue sections from salivary gland biopsies of patients with SS were stained with human anti-150-kd α-fodrin Fab SK415 (**A**, green) and mouse anti-α-fodrin mAb AA6 (**B**, red) and analyzed by laser-scanning confocal microscopy. Intense staining corresponding to acinar epithelia cells, and with intensification at the cell surface was observed with SK415 (**solid arrows**). Only partial co-localization was observed between Fab SK415 and mAb AA6 (**C**), because Fab SK415, but not mAb AA6, also stained areas corresponding to the lymphocytic infiltrate surrounding the affected acini (**open arrow**), whereas AA6, but not SK415, stained unaffected ducts (**arrowhead**). Duct cells from a normal salivary gland were stained with AA6, but not, or only weakly, with SK415 (**D**). No staining of the salivary gland tissue sections was observed with the negative control Fab b12 or a fluorescein isothiocyanate-labeled anti-human $F(ab)_2$ alone (not shown).

Discussion

Lymphocyte infiltration in the salivary glands leading to glandular destruction is a common finding in SS patients. The infiltrate consists of predominantly T cells as well as large numbers of B and plasma cells that actively produce immunoglobulin with autoimmune reactivity. To elucidate the components of this immunopathology, we examined the Ab response to α-fodrin in SS patients using serology and phage display cloning.

In the initial study proposing anti-α-fodrin Abs as a disease marker of SS, Western blot analysis of a large panel of Japanese SS patients showed that IgG Ab to 120-kd cleaved α-fodrin could be used as a marker for SS, because it exhibited high sensitivity (95%) and specificity (100%).[7] Subsequently, anti-120-kd α-fodrin Abs were also found in some patients with SLE without SS.[9] The high sensitivity and specificity of anti-α-fodrin Ab as a diagnostic marker of SS has been questioned,[21] although other investigators have also found good correlation between SS and anti-α-fodrin Abs, although the sensitivity was lower than in the Japanese study.[11,37] We investigated a panel of SS patients fulfilling the strict San Diego criteria by evaluating serum panels by both ELISA and Western blotting using purified mouse brain α-fodrin, similar to the antigen source used in the initial Japanese study. This antigen preparation contains both intact (240 kd) and cleaved forms (eg, 120 kd, 150 kd) of α-fodrin, and thus will also be recognized by Abs that specifically bind epitopes accessible only on the cleaved forms of α-fodrin, such as those cloned in this study. Our study demonstrated significant differences in sensitivity between ELISA and Western blotting, suggesting that a major part of the α-fodrin Ab response is directed against conformational epitopes, or that the affinity of the anti-α-fodrin Ab in some SS patients was not sufficient to allow detection by Western blotting. Nearly all (98%) of the SS patients were positive for α-fodrin by ELISA, whereas anti-α-fodrin Ab reactivity by Western blotting was significantly lower (52%), and only 36.0% stained the 120-kd α-fodrin fragment. Some differences in α-fodrin Ab profiles were observed between the American and the Japanese SS patient groups, probably because the two groups represent two distinct populations with different genetic and environmental influences.

Interestingly, we found that ~25% of both the American and Japanese SS sera recognized a 150-kd fragment of cleaved α-fodrin, an Ab specificity not previously evaluated. This specificity was not seen in a panel of sera from healthy individuals and patients with SLE or RA. Molecular analysis of the anti-150-kd Ab response using IgG Ab phage display libraries generated from two of anti-150-kd seropositive SS patients yielded a panel of hmAbs that specifically recognized the 150-kd form of cleaved α-fodrin and not 120-kd or intact α-fodrin. The specificity of these hmAbs is distinct from that of the currently available mouse anti-α-fodrin mAbs recognizing 150-kd α-fodrin, which also bind 120-kd α-fodrin and intact α-fodrin.

In the NFS/*sld* SS mouse model, dysregulation of anti-fodrin $CD4^+$ T cells leads to Fas-mediated apoptosis of salivary gland epithelial cells and a corresponding increase in clinical symptoms.[8] In humans, a similar scenario has been proposed, and increased apoptosis has been observed in SS salivary glands. Fas expression in the salivary gland cells and FasL on the infiltrating $CD4^+$ T cell in SS patients have been reported, although their roles in disease pathology remain to be elucidated.[38] In addition, CTL-mediated lysis/apoptosis though the granzyme and perforin pathways may be involved in salivary gland destruction.[2] In the mouse model,[8] the increased apoptosis was accompanied by an increase in cleaved 120-kd α-fodrin in the affected tissue, as well as in serum anti-120-kd Ab levels, similar to our observation of cleaved 150-kd α-fodrin in SS patients. Indeed, treatment of mice with caspase inhibitors prevented induction of SS,[19] suggesting that α-fodrin cleavage and anti-α-fodrin Ab production is more that an epiphenomenon. We found the 150-kd α-fodrin fragment within affected acinar epithelial cells, and also in the surrounding lymphocytic infiltrate. In the latter areas, the staining was not confined to cells, suggesting leakage of the 150-kd α-fodrin fragment from the apoptotic acinar/ductal epithelial cells into the surrounding interstitium. Interestingly, leakage of 150-kd fragments of α-fodrin has also been observed in tissue cultures of apoptotic human neuroblastoma

cells.[39] In contrast, the anti-150-kd Fabs stained normal salivary cells with lower intensity than a mouse mAb recognizing both intact and cleaved α-fodrin. Our observation seems to support earlier findings that low levels of 120-kd and 150-kd are present in normal cells, but are significantly increased during apoptosis.[14] Our study also suggests that 150-kd α-fodrin is translocated to cell surface blebs in apoptotic HSG cells, similar to Ro/SSA,[35,36] thereby possibly presenting it to the immune system and eliciting an Ab response. Previous studies have shown α-fodrin to be cleaved by calpain in apoptotic T cells, and by calpain and caspases in anti-Fas-stimulated Jurkat cells and/or neuronal apoptosis.[15–17] In human SS, the 150-kd α-fodrin fragments are most likely the result of caspase cleavage,[18,19] but this requires further analysis. In addition, α-fodrin can be cleaved by an unidentified protease present in granules of $CD8^+$ CTLs.[18] Interestingly, membrane blebbing during apoptosis has been suggested to be partially due to fodrin cleavage.[14]

In conclusion, our data supports the theory that in SS patients, α-fodrin is cleaved during apoptosis in the inflamed salivary gland tissue and elicits an Ab response to the cleaved products. Our study also showed that the Ab response to α-fodrin in SS patients is not limited to Abs against the 120-kd fragment, but includes other cleaved products, such as the 150-kd fragment. Inclusion of these Ab specificities would likely increase the sensitivity of the anti-α-fodrin Ab test, and enhance its usefulness as a diagnostic marker of human SS. The isolated human monoclonal Abs to cleaved α-fodrin may serve as useful reagents for diagnostic immunohistochemical analysis of SS salivary gland tissue and study of SS pathogenesis.

References

1. Fox RI, Tornwall J, Maruyama T, Stern M: Evolving concepts of diagnosis, pathogenesis, and therapy of Sjogren's syndrome. Curr Opin Rheumatol 1998, 10:446–456
2. Tapinos NI, Polihronis M, Tzioufas AG, Skopouli FN: Immunopathology of Sjogren's syndrome. Ann Med Interne (Paris) 1998, 149:17–24
3. Jonsson R, Moen K, Vestrheim D, Szodoray P: Current issues in Sjogren's syndrome. Oral Dis 2002, 8:130–140
4. Fox R: Sjögren's Syndrome: Primer on the Rheumatic Diseases. Atlanta, Arthritis Foundation, 1998, pp 283–286
5. Vitali C, Bombardieri S, Moutsopoulos HM, Balestrieri G, Bencivelli W, Bernstein RM, Bjerrum KB, Braga S, Coll J, de Vita S, et al: Preliminary criteria for the classification of Sjogren's syndrome. Results of a prospective concerted action supported by the European Community. Arthritis Rheum 1993, 36:340–347
6. Vitali C, Bombardieri S, Moutsopoulos HM, Coll J, Gerli R, Hatron PY, Kater L, Konttinen YT, Manthorpe R, Meyer O, Mosca M, Ostuni P, Pellerito RA, Pennec Y, Porter SR, Richards A, Sauvezie B, Schiodt M, Sciuto M, Shoenfeld Y, Skopouli FN, Smolen JS, Soromenho F, Tishler M, Wattiaux MJ: Assessment of the European classification criteria for Sjogren's syndrome in a series of clinically defined cases: results of a prospective multicentre study. The European Study Group on Diagnostic Criteria for Sjogren's Syndrome. Ann Rheum Dis 1996, 55: 116–121
7. Haneji N, Nakamura T, Takio K, Yanagi K, Higashiyama H, Saito I, Noji S, Sugino H, Hayashi Y: Identification of alpha-fodrin as a candidate autoantigen in primary Sjogren's syndrome. Science 1997, 276: 604–607
8. Ishimaru N, Saegusa K, Yanagi K, Haneji N, Saito I, Hayashi Y: Estrogen deficiency accelerates autoimmune exocrinopathy in murine Sjogren's syndrome through Fas-mediated apoptosis. Am J Pathol 1999, 155:173–181
9. Watanabe T, Tsuchida T, Kanda N, Mori K, Hayashi Y, Tamaki K: Anti-alpha-fodrin antibodies in Sjogren syndrome and lupus erythematosus. Arch Dermatol 1999, 135:535–539
10. Miyagawa S, Yanagi K, Yoshioka A, Kidoguchi K, Shirai T, Hayashi Y: Neonatal lupus erythematosus: maternal IgG antibodies bind to a recombinant NH2-terminal fusion protein encoded by human alpha-fodrin cDNA. J Invest Dermatol 1998, 111:1189–1192
11. Witte T, Matthias T, Oppermann M, Helmke K, Peter HH, Schmidt RE, Tishler M: Prevalence of antibodies against alpha-fodrin in Sjogren's syndrome: comparison of 2 sets of classification criteria. J Rheumatol 2003, 30:2157–2159
12. Perrin D, Aunis D: Reorganization of alpha-fodrin induced by stimulation in secretory cells. Nature 1985, 315:589–592
13. Leto TL, Pleasic S, Forget BG, Benz Jr EJ, Marchesi VT: Characterization of the calmodulin-binding site of nonerythroid alpha-spectrin. Recombinant protein and model peptide studies. J Biol Chem 1989, 264:5826–5830
14. Martin SJ, O'Brien GA, Nishioka WK, McGahon AJ, Mahboubi A, Saido TC, Green DR: Proteolysis of fodrin (non-erythroid spectrin) during apoptosis. J Biol Chem 1995, 270:6425–6428
15. Martin SJ, Finucane DM, Amarante-Mendes GP, O'Brien GA, Green DR: Phosphatidylserine externalization during CD95-induced apoptosis of cells and cytoplasts requires ICE/CED-3 protease activity. J Biol Chem 1996, 271:28753–28756
16. Vanags DM, Porn-Ares MI, Coppola S, Burgess DH, Orrenius S: Protease involvement in fodrin cleavage and phosphatidylserine exposure in apoptosis. J Biol Chem 1996, 271:31075–31085
17. Nath R, Raser KJ, Stafford D, Hajimohammadreza I, Posner A, Allen H, Talanian RV, Yuen P, Gilbertsen RB, Wang KK: Non-erythroid alpha-spectrin breakdown by calpain and interleukin 1 beta-converting-enzyme-like protease(s) in apoptotic cells: contributory roles of both protease families in neuronal apoptosis. Biochem J 1996, 319:683–690
18. Nagaraju K, Cox A, Casciola-Rosen L, Rosen A: Novel fragments of the Sjogren's syndrome autoantigens alpha-fodrin and type 3 muscarinic acetylcholine receptor generated during cytotoxic lymphocyte granule-induced cell death. Arthritis Rheum 2001, 44:2376–2386
19. Saegusa K, Ishimaru N, Yanagi K, Mishima K, Arakaki R, Suda T, Saito I, Hayashi Y: Prevention and induction of autoimmune exocrinopathy is dependent on pathogenic autoantigen cleavage in murine Sjogren's syndrome. J Immunol 2002, 169:1050–1057
20. Maeno N, Takei S, Imanaka H, Oda H, Yanagi K, Hayashi Y, Miyata K: Anti-alpha-fodrin antibodies in Sjogren's syndrome in children. J Rheumatol 2001, 28:860–864
21. Witte T, Matthias T, Arnett FC, Peter HH, Hartung K, Sachse C, Wigand R, Braner A, Kalden JR, Lakomek HJ, Schmidt RE: IgA and IgG autoantibodies against alpha-fodrin as markers for Sjogren's syndrome. Systemic lupus erythematosus. J Rheumatol 2000, 27: 2617–2620
22. Yanagi K, Ishimaru N, Haneji N, Saegusa K, Saito I, Hayashi Y: Anti-120-kDa alpha-fodrin immune response with Th1-cytokine profile in the NOD mouse model of Sjogren's syndrome. Eur J Immunol 1998, 28:3336–3345
23. Fox RI, Saito I: Criteria for diagnosis of Sjögren's syndrome. Rheum Dis Clin North Am 1994, 20:391–407
24. Cheney R, Levine J, Willard M: Purification of fodrin from mammalian brain. Methods Enzymol 1986, 134:42–54
25. Janicke RU, Ng P, Sprengart ML, Porter AG: Caspase-3 is required for alpha-fodrin cleavage but dispensable for cleavage of other death substrates in apoptosis. J Biol Chem 1998, 273:15540–15545
26. Chomczynski P, Sacchi N: Single-step method of RNA isolation by acid guanidinium thiocyanate-phenol-chloroform extraction. Anal Biochem 1987, 162:156–159
27. Persson MA, Caothien RH, Burton DR: Generation of diverse high-affinity human monoclonal antibodies by repertoire cloning. Proc Natl Acad Sci USA 1991, 88:2432–2436
28. Barbas III CF, Wagner J: Synthetic human antibodies selecting and evolving functional protein. Methods CTMIE 1995, 8:94–103
29. Burton DR, Barbas III CF, Persson MA, Koenig S, Chanock RM, Lerner RA: A large array of human monoclonal antibodies to type 1 human immunodeficiency virus from combinatorial libraries of asymptomatic seropositive individuals. Proc Natl Acad Sci USA 1991, 88: 10134–10137

30. Maruyama T, Rodriguez LL, Jahrling PB, Sanchez A, Khan AS, Nichol ST, Peters CJ, Parren PW, Burton DR: Ebola virus can be effectively neutralized by antibody produced in natural human infection. J Virol 1999, 73:6024–6030
31. Warmerdam PA, van den Herik-Oudijk IE, Parren PW, Westerdaal NA, van de Winkel JG, Capel PJ: Interaction of a human Fc gamma RIIb1 (CD32) isoform with murine and human IgG subclasses. Int Immunol 1993, 5:239–247
32. Ditzel HJ, Binley JM, Moore JP, Sodroski J, Sullivan N, Sawyer LS, Hendry RM, Yang WP, Barbas III CF, Burton DR: Neutralizing recombinant human antibodies to a conformational V2- and CD4-binding site-sensitive epitope of HIV-1 gp120 isolated by using an epitope-masking procedure. J Immunol 1995, 154:893–906
33. Binley JM, Ditzel HJ, Barbas III CF, Sullivan N, Sodroski J, Parren PW, Burton DR: Human antibody responses to HIV type 1 glycoprotein 41 cloned in phage display libraries suggest three major epitopes are recognized and give evidence for conserved antibody motifs in antigen binding. AIDS Res Hum Retroviruses 1996, 12:911–924
34. Casciola-Rosen LA, Anhalt G, Rosen A: Autoantigens targeted in systemic lupus erythematosus are clustered in two populations of surface structures on apoptotic keratinocytes. J Exp Med 1994, 179: 1317–1330
35. Baboonian C, Venables PJ, Booth J, Williams DG, Roffe LM, Maini RN: Virus infection induces redistribution and membrane localization of the nuclear antigen La (SS-B): a possible mechanism for autoimmunity. Clin Exp Immunol 1989, 78:454–459
36. Bachmann M, Chang S, Slor H, Kukulies J, Muller WE: Shuttling of the autoantigen La between nucleus and cell surface after UV irradiation of human keratinocytes. Exp Cell Res 1990, 191:171–180
37. Zandbelt M, Degen W, van de Putte L, van Venrooij W, van den Hoogen Nijmegen F: Anti-a-fodrin antibodies: not specific nor sensitive for Sjögren's syndrome. Arthritis Rheum 1999, 42(Abstract 428 Suppl):S142
38. Kong L, Ogawa N, Nakabayashi T, Liu GT, D'Souza E, McGuff HS, Guerrero D, Talal N, Dang H: Fas and Fas ligand expression in the salivary glands of patients with primary Sjogren's syndrome. Arthritis Rheum 1997, 40:87–97
39. Dutta S, Chiu YC, Probert AW, Wang KK: Selective release of calpain produced alphall-spectrin (alpha-fodrin) breakdown products by acute neuronal cell death. Biol Chem 2002, 383:785–791

0013-7227/04/$15.00/0
Printed in U.S.A.

Endocrinology 145(5):2384–2391

doi: 10.1210/en.2003-1536

Estrogen Deficiency Accelerates Murine Autoimmune Arthritis Associated with Receptor Activator of Nuclear Factor-κB Ligand-Mediated Osteoclastogenesis

TOMOKO YONEDA, NAOZUMI ISHIMARU, RIEKO ARAKAKI, MASARU KOBAYASHI, TAKASHI IZAWA, KEIJI MORIYAMA, AND YOSHIO HAYASHI

Departments of Pathology (T.Y., N.I., R.A., M.K., T.I., Y.H.) and Orthodontics (T.Y., T.I., K.M.), Tokushima University School of Dentistry, Tokushima 770-8504 Japan

The aims of this study were to evaluate the *in vivo* effects of estrogen deficiency in MRL/*lpr* mice as a model for rheumatoid arthritis and to analyze the possible relationship between immune dysregulation and receptor activator of nuclear factor-κB ligand (RANKL)-mediated osteoclastogenesis. Experimental studies were performed in ovariectomized (Ovx)-MRL/*lpr*, Ovx-MRL+/+, sham-operated-MRL/*lpr*, and sham-operated-MRL+/+ mice. Severe autoimmune arthritis developed in younger Ovx-MRL/*lpr* mice until 24 wk of age, whereas these lesions were entirely recovered by pharmacological levels of estrogen administration. A significant elevation in serum rheumatoid factor, anti-double-stranded DNA, and anti-type II collagen was found in Ovx-MRL/*lpr* mice and recovered in mice that underwent estrogen administration. A high proportion of $CD4^+$ T cells bearing RANKL was found, and an enhanced expression of RANKL mRNA and an impaired osteoprotegerin mRNA was detected in the synovium. An increase in both osteoclast formation and bone resorption pits was found. These results indicate that estrogen deficiency may play a crucial role in acceleration of autoimmune arthritis associated with RANKL-mediated osteoclastogenesis in a murine model for rheumatoid arthritis. (*Endocrinology* 145: 2384–2391, 2004)

IT IS WELL KNOWN that sex steroids have significant impact on the development of autoimmune diseases in both humans and rodents. In particular, estrogen has been suggested to be responsible for the strong female preponderance of the human rheumatoid arthritis (RA), systemic lupus erythematosus, scleroderma, and Sjögren's syndrome (1–3), but the role of estrogens in the female has not been fully characterized. RA is a chronic inflammatory disease characterized by invasive synovial hyperplasia leading to progressive joint destruction. Rheumatoid synovial cells are not only morphologically characterized by their transformed appearance (4) but also are phenotypically transformed to proliferate abnormally (5, 6). These cells invade bone and cartilage by producing an elevated amount of proinflammatory cytokines (7) and matrix metalloproteinases (MMPs) (8) and by inducing osteoclast (OC) formation and activation (9, 10).

OCs, the multinucleated cells exclusively responsible for bone resorption, have been observed to resorb bone actively at the site of invasion of the proliferated synovial membrane into the adjacent bone (11). The cell types responsible for bone resorption in RA have been characterized as authentic OCs (12), and it was reported that rheumatoid synovial fibroblasts are involved in bone destruction by inducing osteoclastogenesis (13). However, the exact mechanisms involved in the formation and activation of OCs in RA are still unclear.

Receptor activator of nuclear facto-κB ligand (RANKL) (14) is a regulator of the immune system and of bone development (15). RANKL is expressed on activated T cells (16), and a major target for RANKL in the immune system appears to be mature dendritic cells (DCs) that express a high level of RANKL receptor (RANK) (17). *In vitro*, RANKL promotes the survival of mature DCs, most likely by up-regulating the expression of Bcl-XL (18), and induces the production of proinflammatory cytokines, such as IL-1 and IL-6, and cytokines that stimulate and induce differentiation of T cells, such as IL-12 and IL-15 (19). Therefore, RANKL is likely to act as a positive-feedback regulator during productive T cell-DC interactions (20).

The MRL/*lpr* mouse strain was chosen to test the estrogenic action because it has a genetic predisposition to arthritis with characteristics similar to those of human RA including cell infiltration, pannus formation, bone and cartilage breakdown, and the presence of serum rheumatoid factor (RF) (21–23). The aim of this study was to analyze the *in vivo* effects of estrogen deficiency on the development of autoimmune arthritis in MRL/*lpr* mice and to evaluate the possible relationship with RANKL-mediated osteoclastogenesis.

Materials and Methods

Mice and treatment

MRL/Mp-*lpr*/*lpr* (MRL/*lpr*, age 4–24 wk; n = 108) and MRL+/+ mice (age 4–24 wk; n = 58) were purchased from Charles River Japan

Abbreviations: Ab, Antibody; CII, type 2 collagen; DC, dendritic cell; dsDNA, double-stranded DNA; ER, estrogen receptor; IFN, interferon; IRF, IFN regulatory factor; LN, lymph node; mAb, monoclonal antibody; MMP, matrix metalloproteinase; OC, osteoclast; OPG, osteoprotegerin; Ovx, ovariectomized; RA, rheumatoid arthritis; RANK, RANKL receptor; RANKL, receptor activator of nuclear factor-κB ligand; RF, rheumatoid factor; sham, sham-operated; TRAP, tartrate-resistant acid phosphatase.

Endocrinology is published monthly by The Endocrine Society (http://www.endo-society.org), the foremost professional society serving the endocrine community.

Inc. (Atsugi, Japan), and were fed under specific pathogen-free conditions. Female MRL/*lpr* mice and MRL+/+ mice (4 wk of age) were ovariectomized (Ovx) and compared with sham-operated (sham)-MRL/*lpr* and MRL+/+ mice. Six to 10 mice in each group were analyzed at 8, 12, 16, 20, and 24 wk of age. Ovx-MRL/*lpr* mice were administered im with 60 mg/kg·wk estrogen (Ovahormine depo; Teikoku Zouki Inc., Tokyo, Japan) in sesame oil or sc with 25 mg/kg·d testosterone (Wako Pure Chemical, Osaka, Japan) from 4–20 wk of age. Care of the mice was in accordance with institutional guidelines.

Histology and immunohistology

All organs were removed from the mice and fixed with 10% phosphate-buffered formalin, and ankles were further decalcified in 10% EDTA. Sections (4 μm in thickness) were stained with hematoxylin and eosin. Histological grading of inflammatory arthritis was done according to the methods by Edwards *et al.* (24) as follows: one point score indicates hyperplasia/hypertrophy of synovial cells; fibrosis/fibroplasia; proliferation of cartilage and bone; destruction of cartilage and bone; and/or mononuclear cell infiltrate. Immunohistological analysis was performed on freshly frozen sections (4 μm in thickness) by the biotin-avidin immunoperoxidase method using ABC reagent (Vector Laboratories Inc., Burlingame, CA). The monoclonal antibodies (mAb) used were biotinylated rat mAbs to CD4, CD8 (BD Biosciences, San Jose, CA), and mouse RANKL (IMGENEX, San Diego, CA).

Flow cytometric analysis

Spleen and inguinal lymph node (LN) cell suspensions were stained with antibodies (Ab) conjugated to phycoerythrin (anti-CD4, Cedarlane Laboratories Ltd., Ontario, Canada; B220, PharMingen, San Diego, CA), fluorescein isothiocyanate (anti-CD8, Cedarlane Laboratories; Thy1.2, PharMingen), and antimouse RANKL (IMGENEX) and analyzed with EPICS (Coulter, Miami, FL).

Measurement of anti-double-stranded DNA (dsDNA) Ab, RF, and type 2 collagen (CII) Ab levels

Anti-dsDNA Abs, RF, and anti-CII Ab were detected by ELISA as described previously (25–27). Briefly, flat-bottom plates (Nalge Nunc International, Roskilde, Denmark) were coated with 1.5 μg/ml of native calf thymus DNA (Life Technologies, Inc., Rockville, MD) in buffer containing 0.1 M sodium bicarbonate and 0.05 M citric acid at 4 C overnight. Serum samples were serially diluted (starting at 1/200) and added to the plates for a 1-h incubation at 37 C. After washing, peroxidase-conjugated goat antimouse IgG, or IgM (Southern Biotechnology Associates, Birmingham, AL), was added and incubated for 1 h at 37 C. Ab binding was visualized using orthophenylenediamine (Sigma, St. Louis, MO). For the measurement of IgG and IgM RF, human IgG and IgM (Chemicon International, Temecula, CA) were coated onto plates at 10 μg/ml in carbonate buffer, and the same procedures were followed as described above. For the measurement of serum Abs to CII, native bovine CII was dissolved in 0.1 M acetic acid at 1 mg/ml and diluted with 0.1 M sodium bicarbonate at 10 μg/ml (pH 9.6). The microtiter plate was coated with 100 μl of CII antigen solution. After washing three times, 100 μl per well of serum samples that had been serially diluted in PBS/Tween 20/1% BSA and control serum were added and incubated for 1 h at 37 C. After washing, peroxidase-conjugated goat antimouse IgG (at 1.4 μg/ml, 100 μl per well) (Organon Teknika, Durham, NC) was added and incubated for 1 h at 37 C. A total of 100 μl o-phenylenediamine (0.5 mg/ml) dissolved in 0.1 M citrate buffer (pH 5.0) containing 0.012% H_2O_2 was added, and the reaction was stopped using 8 N H_2SO_4 (20 μl per well).

Measurement of cytokine production

Cytokine production was tested by two-step sandwich ELISA using a mouse IL-2, IL-4, and interferon (IFN)-γ kit (Genzyme, Cambridge, MA). In brief, culture supernatants from LN cells activated with immobilized anti-CD3 mAb (Cedarlane Laboratories) for 3 d were added to microtiter plates precoated with anti-IL-2, IL-4, and IFN-γ capture Ab and incubated overnight at 4 C. After addition of biotinylated detecting Ab and incubation at room temperature for 45 min, avidin-peroxidase was added and incubated at room temperature for 30 min. Finally, 2,2′-azino-di-3-ethylbenzthiazoline sulfonate substrate containing H_2O_2 was added, and the colorimetric reaction was read at an absorbance of 405 nm using an automatic microplate reader (Bio-Rad Laboratories Inc., Hercules, CA). The concentrations of IL-2 (picograms per milliliter), IL-4 (picograms per milliliter), and IFN-γ (picograms per milliliter) were calculated according to the standard curves produced by various concentrations of recombinant cytokines.

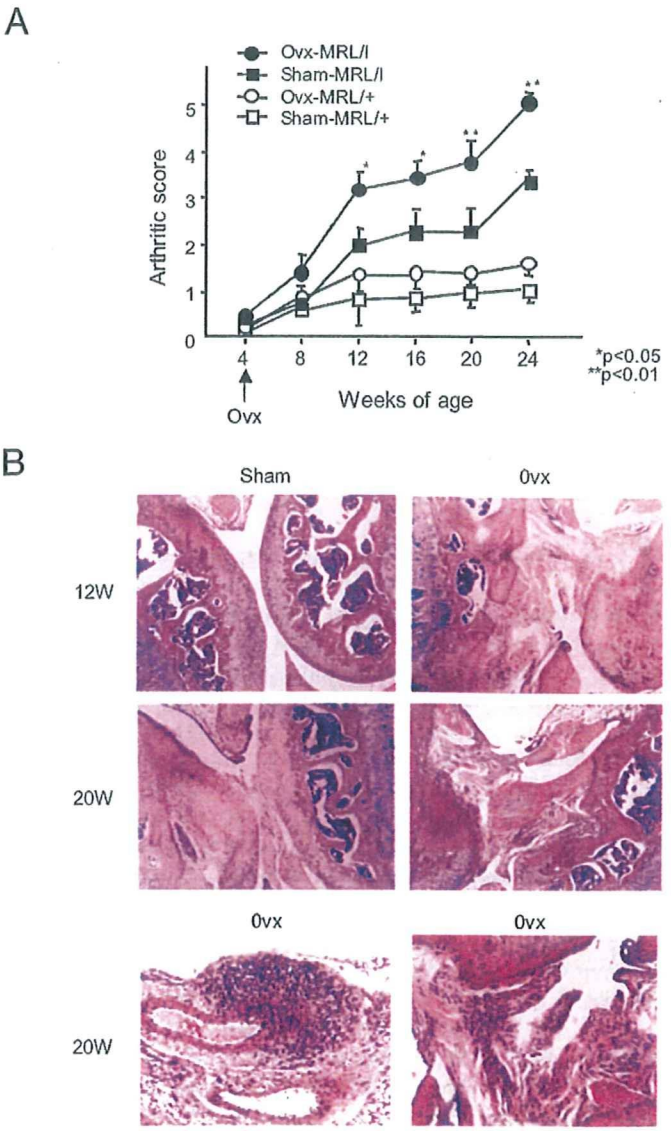

FIG. 1. Effects of the Ovx on joint histopathology. Histological score of autoimmune arthropathy developed in younger Ovx-MRL/*lpr* mice compared with those in sham-MRL/*lpr* and Ovx-MRL+/+ mice until 24 wk of age (A). Histological evaluation of the knee joints was performed according to the methods by Edwards *et al.* (24) (*, $P < 0.05$; and **, $P < 0.01$, Student's t test). Representative photomicrographs taken from Ovx- and sham-MRL/*lpr* mice at 12 (12W) and 20 wk (20W) of age (B). The histopathological effects observed in Ovx-MRL/*lpr* mice at age 20 wk included mononuclear cell infiltration into the subsynovial tissue (*lower left*), and synovial hyperplasia (*lower right*) (hematoxylin and eosin). In contrast, mononuclear cell infiltration and bone and cartilage pathology was absent in sham-MRL/*lpr* mice until 20 wk of age (*middle left*).

ELISA for murine osteoprotegerin (OPG)

An anti-murine OPG mAb (TECHNE Corp., Minneapolis, MN) was diluted with 0.1 M sodium bicarbonate (pH 9.6) solution to a concentration of 10 μg/ml, and the 100-μl aliquot was added to each well of 96-well plates. After incubation at 4 C overnight, the capture solution was removed by flicking the plates, and the wells were blocked with the blocking solution (300 μl per well) for 2 h at room temperature. Recombinant OPG (100 μl) (R&D System Inc., Minneapolis, MN) standard and a series of test samples were added to the wells, and the plates were incubated for 2 h at room temperature. The wells were then washed with the washing buffer, and 100 μl of peroxidase-labeled anti-OPG mAb was added to each well. After incubation for an additional 2 h, 100 μl of tetramethylbenzidine substrate reagent was added to each well. Tetramethylbenzidine stop buffer (100 μl) was added to each well, and absorbance at 450 nm of the wells was measured with a microplate reader (Bio-Rad Laboratories Inc.).

RT-PCR

The total RNA from LNs and synovial tissues was extracted as reported previously (28). The RNA was reverse-transcribed into cDNA. The cDNA reaction mixture was diluted with 90 μl of PCR buffer and mixed with 500 nM of the 5′ and 3′ primers, 0.1 mM deoxynucleotide triphosphate mix, 2 mM $MgCl_2$, and 2 U thermostable *Taq* polymerase (PerkinElmer Cetus, Norwalk, CT). The cDNA was subjected to enzymatic amplification in a DNA thermal cycler (PerkinElmer Cetus) by using specific primers. PCR was carried out at 55 C annealing temperature for 30–35 cycles. The specific primers used were as follows: IL-1β, TGA TGA GAA TGA CCT GTT CT and CTT CTT CAA AGA TGA AGG AAA; TNF-α, ATG AGC ACA GAA AGC ATG ATC and AGA TGA TCT GAG TGT GAG GG; IL-6, CTC TGC AAG AGA GAC TTC CAT and ATA GGC AAA TTT CCT GAT TAT A; IFN-γ, CCT CAG ACT CTT TGA ACT CT and CAG CGA CTC CTT TTC CGC TT; IFN regulatory factor (IRF)-1, TCT GAG TGG CAT ATG CAG ATG GAC and GGT CAG AGA CCC AAA CTA TGG TCG; MMP-1, ATG GTG GGG ATG CCC ATT TT and CAG CAT CTA CTT TGT TGC C; MMP-2, GAG TTG GCA GTG CAA TAC CT and GCC ATC CTT CTC AAA GTT GT; MMP-3, GAA ATG CAG AAG TTC CTC GG and GAG TTC CAT AGA GGG ACT GA; MMP-9, CCA TGA GTC CCT GGC AG and AGT ATG TGA TGT TAT GAT G; TIMP (tissue inhibitor of metalloproteinase)-1, CTG GCA TCC TCT TGT TGC TA and AGG GAT CTC CAA GTG CAC AA; RANKL, GGG AAT TAC AAA GTG CAC CAG and GCC ATC CTT CTC AAA GTT GT; RANK, GTC TTC TGG AAC CAT CTT CTC C and CAC AGA CAA ATG CAA ACC TTG; OPG, TCA AGT GCT TGA GGG CAT AC and TGG AGA TCG AAT TCT GCT TG; estrogen receptor (ER)-α, AAT TCT GAC AAT CGA CGC CAG and GTG CTT CAA CAT TCT CCC TCC TC; ER-β, TTC CCA GCA GCA CCG GTA ACC T and TCC CTC TTG GCG CTT GGA CTA; β-actin, GTG GGC CGC TCT AGG CAC CA and CGG TTG GCC TTA GGG TTC AGG GGG. The amplified DNA reaction mixture was subjected to 1.7% agarose gel electrophoresis, and the amplified product was visualized by UV fluorescence after staining with ethidium bromide.

Tartrate-resistant acid phosphatase (TRAP) staining

Staining for TRAP was performed according to the modified method of Takahashi *et al.* (29). Sections were rinsed once with PBS (pH 7.4), air dried, fixed with 10% formalin in PBS (pH 5.4) for 5 min, and fixed with

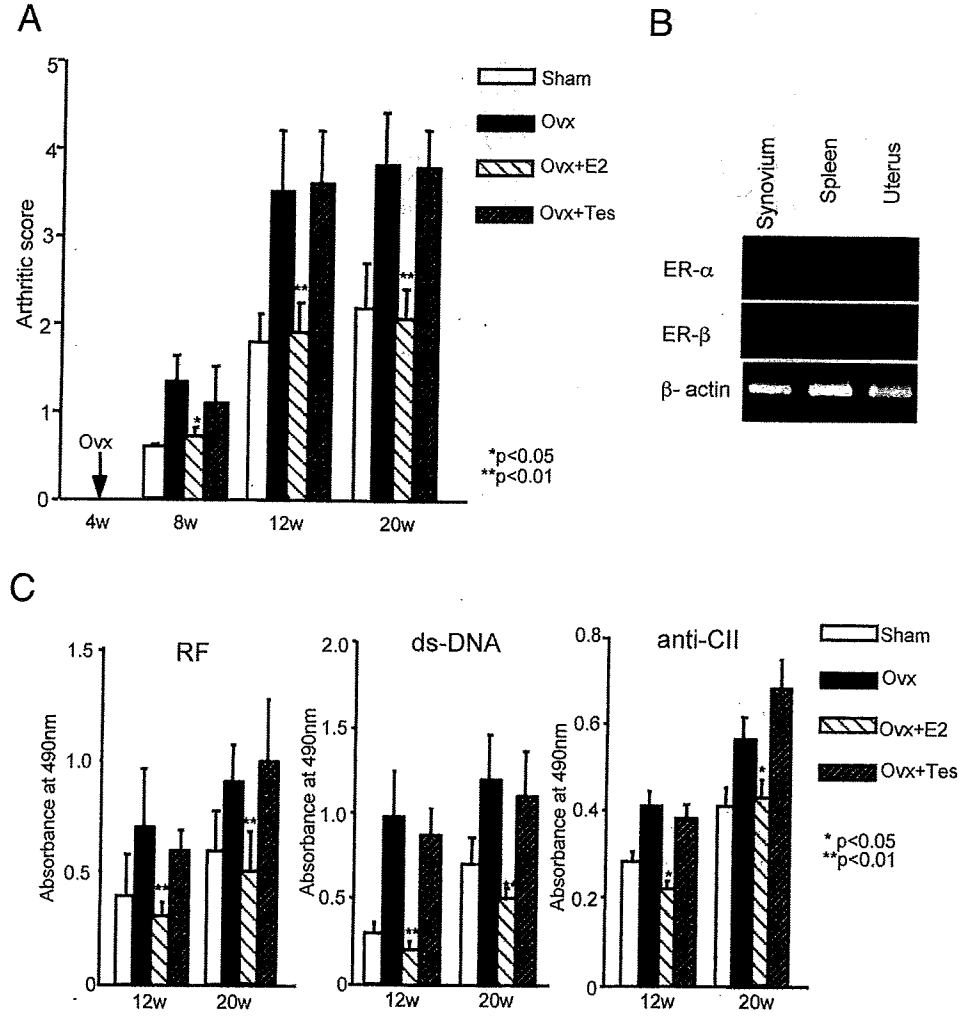

FIG. 2. The destructive lesions in the knee joints in Ovx-MRL/*lpr* mice were inhibited by estrogen administration (10^{-9} M) at ages 12 and 20 wk (*, $P < 0.05$ and **, $P < 0.01$, Student's *t* test) (A). Detection of gene expression in ER-α in the synovium but not in ER-β by RT-PCR analysis (B). E2, 17β-Estradiol. Serum RF, anti-dsDNA Abs, and anti-CII were significantly increased in Ovx-MRL/*lpr* mice compared with those in sham-MRL/*lpr* mice, and these changes were entirely recovered by the treatment with estrogen administration (10^{-9} M) at 12 and 20 wk of age (*, $P < 0.05$; and **, $P < 0.01$, Student's *t* test) (C). Tes, Testosterone.

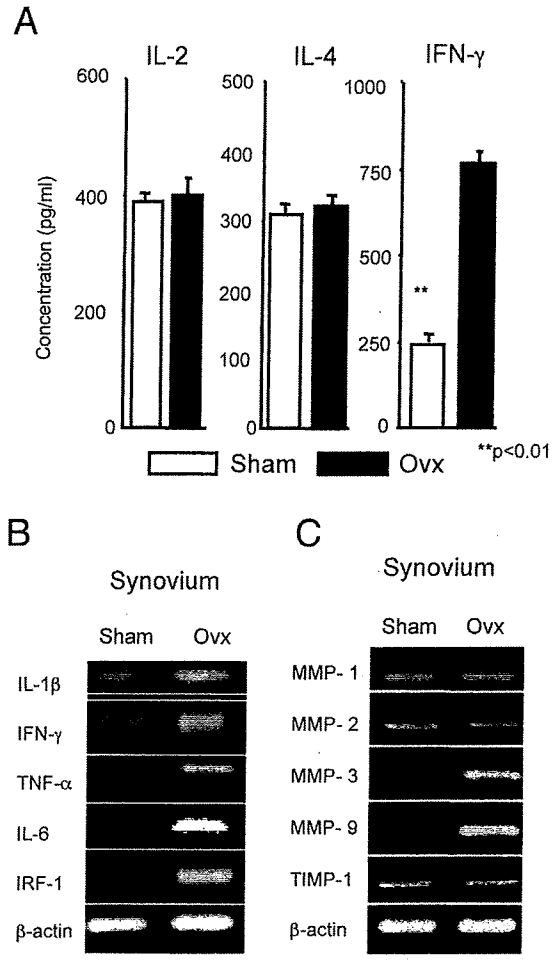

FIG. 3. Effects of the Ovx on expression of cytokines and MMPs. Culture supernatants from anti-CD3 mAb-stimulated LN T cells obtained from Ovx-MRL/*lpr* mice at age 20 wk contained high levels of IFN-γ (**, $P < 0.01$, Student's t test), whereas no different levels of IL-2 and IL-4 was observed by ELISA (A). Increased expressions of cytokine genes including IL-1β, IFN-γ, TNF-α, IL-6, IRF-1, and β-actin were detected in synovium from Ovx-MRL/*lpr* mice at age 20 wk, compared with those from sham-mice by RT-PCR analysis (B). Enhanced gene expressions of MMP-3, and MMP-9 mRNA were found in synovium from Ovx-MRL/*lpr* mice at age 20 wk (C).

methanol-acetone (50:50; pH 5.4) for 30 sec. The coverslips were air-dried and stained for 15 min at room temperature in a 0.1 M sodium acetate buffer (pH 5.0) containing naphthol AS-MX phosphate (Sigma) as a substrate and fast red violet LB salt (Sigma) as a stain for the reaction product in the presence of 50 mM of sodium tartrate.

Assessment of bone resorption

Bone marrow cells (5×10^5) from Ovx- and sham-MRL/*lpr* mice were added to the wells of 96-well plates containing a slice of bovine cortical bone and incubated in a total volume of 200 μl α-MEM-fetal bovine serum as described previously (30). All cultures were maintained in the presence of dexamethazone (10^{-7} M, FUNAKOSHI Pharmcol., Tokyo, Japan) and 1α,25-$(OH)_2D_3$ (10^{-8} M, Chugai Inc., Tokyo, Japan) for 10 d. Bone slices were assessed for bone resorptive activity, brushed with a rubber policeman to remove cells after observation under a microscope, and stained with Mayer's hematoxylin. Bone resorption pits were quantified by densitometric analysis of images of the whole area of bone slices as previously described (30). Additionally, *in vitro* osteoclastogenesis was assayed using bone marrow-derived TRAP-positive cells with macrophage colony stimulating factor (5 ng/ml; PeproTech EC, London, UK), recombinant murine RANKL (10 ng/ml; PeproTech Inc., Rocky Hill, NJ), recombinant OPG (100 ng/ml; R&D Systems Inc.), and 17β-estradiol (10^{-9} M), at indicated concentration after the estimation of dose responses.

Results

Effects of the Ovx on joint histopathology

Destructive autoimmune arthritis developed in young Ovx-MRL/*lpr* mice, not in young sham-MRL/*lpr* and Ovx-MRL+/+ mice, and these lesions aggravated with age from 12 until 24 wk of age. Histological analysis of the knee joints was performed at 8, 12, 16, 20, and 24 wk of age for all the experiments. Analysis of the histological results for the experiment, shown in Fig. 1A, indicates that the group that was treated with Ovx had significant higher subsynovial inflammation, synovial hyperplasia, pannus formation and cartilage erosion, bone destruction, and overall histopathology. Shown in Fig. 1B are photomicrographs taken from representative Ovx- and sham-MRL/*lpr* mice at 12 and 20 wk of age. The effects observed in Ovx-MRL/*lpr* mice included synovial hyperplasia, pannus formation, bone erosion, and infiltration of mononuclear cells into the subsynovial tissue. In contrast, mononuclear cell infiltration and bone and cartilage pathology was absent in sham-MRL/*lpr* mice until age 20 wk.

Recovery of autoimmune arthritis by estrogen administration

The destructive lesions in the knee joints in Ovx-MRL/*lpr* mice were inhibited by estrogen administration (10^{-9} M) at 12 and 20 wk of age (Fig. 2A). Testosterone administration in Ovx-MRL/*lpr* mice resulted in severe inflammatory lesions as the same levels. We confirmed gene expression in ER-α but not ER-β in synovial tissues by RT-PCR analysis (Fig. 2B), indicating that estrogenic action to the synovial tissues might be directly affected through estrogen/ER-α binding *in vivo*. We detected increased levels of serum RF, anti-dsDNA, and anti-CII Abs in Ovx-MRL/*lpr* mice compared with those in sham mice, and these levels were entirely recovered in Ovx-MRL/*lpr* mice that underwent estrogen administration (Fig. 2C).

Effects of the Ovx on cytokine and MMP expression

Culture supernatants from anti-CD3 mAb-stimulated LN T cells obtained from Ovx-MRL/*lpr* mice at 20 wk of age contained high levels of IFN-γ, whereas no difference in levels of IL-2 and IL-4 was observed by ELISA (Fig. 3A). We next analyzed the effects of the Ovx on various gene expressions in the synovial tissues. Increased expressions of cytokine genes including IL-1β, IFN-γ, TNF-α, IL-6, IRF-1, and β-actin mRNA were detected in synovial tissues from Ovx-MRL/*lpr* mice at 20 wk of age, compared with those from sham-MRL/*lpr* mice by RT-PCR analysis (Fig. 3B). In addition, we found elevated gene expressions of MMP-3 and MMP-9 in synovial tissues from Ovx-MRL/*lpr* mice (Fig. 3C). These data suggest that estrogen deficiency induces various gene expressions directly responsible for tissue damage on the development of autoimmune arthritis.

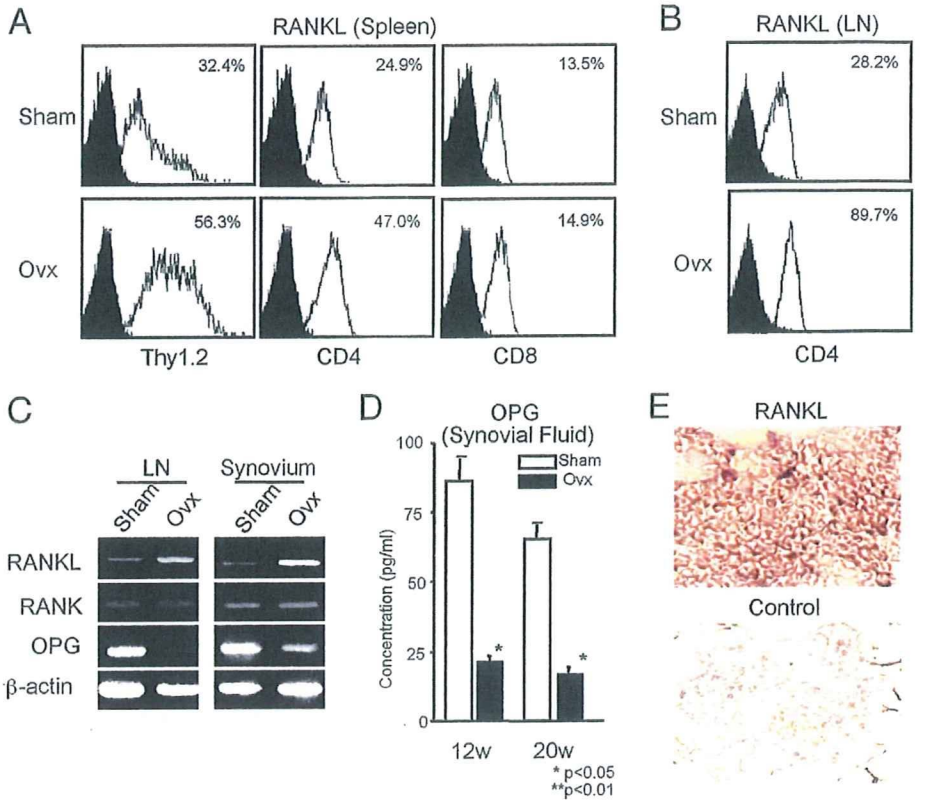

FIG. 4. A significant increase in splenic Thy1.2$^+$ and CD4$^+$ T cells bearing RANKL from Ovx-MRL/lpr mice at 20 wk of age was observed as compared with those from sham-MRL/*lpr* mice, whereas no remarkable change in CD8$^+$ T cells bearing RANKL was found (A). A large proportion of CD4$^+$ T cells in LN bearing RANKL (89.7%) from Ovx-MRL/*lpr* mice was detected on flow cytometry, as compared with that of sham-MRL/*lpr* mice (28.2%) (B). A prominently enhanced RANKL mRNA and an impaired OPG mRNA were observed in LN and synovium from Ovx-MRL/*lpr* mice by RT-PCR analysis (C). A significantly decreased OPG concentration was found in synovial fluid of Ovx-MRL/*lpr* mice at ages 12 (12w) and 20 wk (20w) (*, $P < 0.05$; **, $P < 0.01$, Student's *t* test) (D). A large proportion of infiltrating cells in synovium was positive for RANKL in Ovx-MRL/*lpr* mice at 20 wk of age. Isotype-matched controls were all negative (E).

Effects of the Ovx on RANKL, RANK, and OPG expression

We analyzed the spleen and LN cells bearing RANKL by flow cytometry. A significant increase of Thy1.2$^+$, and CD4$^+$ T cells bearing RANKL in the spleen from Ovx-MRL/*lpr* mice was observed, compared with those from sham-MRL/*lpr* (Fig. 4A). We detected a large proportion of CD4$^+$ T cells in LN bearing RANKL (89.7%) from Ovx-MRL/*lpr* mice as compared with those from sham-MRL/*lpr* mice (28.2%) (Fig. 4B). In addition, an enhanced RANKL mRNA and an impaired OPG mRNA were observed in LN and synovium from Ovx-MRL/*lpr* mice, compared with those in sham-mice by RT-PCR analysis (Fig. 4C). Indeed, a significant decrease in OPG concentration was found in synovial fluid of Ovx-MRL/*lpr* mice compared with those of sham-mice at 12 and 20 wk of age (Fig. 4D). A large proportion of infiltrating cells in synovium was positive for RANKL in Ovx-MRL/*lpr* mice (Fig. 4E).

Effects of the Ovx on OC formation and bone resorption

As seen in Fig. 5A, numerous multinucleated (more than three nuclei), TRAP-positive OC-like cells were detected in the knee joints from both Ovx- and sham-MRL/*lpr* mice. A significant increase in number of OCs formed in the joints from Ovx-MRL/*lpr* mice was observed compared with those from sham-MRL/*lpr* mice (Fig. 5B). We next examined *in vitro* whether the TRAP-positive multinucleated cells (more than three nuclei) from bone marrow cells resorbed bovine bone slices (30). When the bone marrow cells were cultured with dexamethasone and 1α,25-$(OH)_2D_3$, they differentiated into TRAP-positive multinucleated cells, and numerous resorption pits were formed on their surfaces (Fig. 5C). A significantly large number of resorption pits were formed using the bone marrow cells from Ovx-MRL/*lpr* mice compared with those from sham-MRL/*lpr* mice (Fig. 5D).

Discussion

RA is characterized by progressive joint damage that is mediated by several mechanisms (31). Although the etiology of RA remains unknown, joint damage results from the degradation of connective tissue by MMPs and the stimulation of osteoclastogenesis by activated CD4$^+$ T cells (10). Sex hormones influence both humeral and cell-mediated immune response, and estrogen is one of potential factors in this immunological dimorphism (32–34). We have examined the effects of the Ovx on the development of autoimmune arthritis in animals that are susceptible to the development of human RA-like disease. Histology of autoimmune arthritis in Ovx-MRL/*lpr* mice showed severe destructive changes in the younger age examined. It is generally accepted that a severe inflammatory arthritis and systemic autoimmune disease, including glomerulonephritis and autoantibody production, develop in aged (>6-month-old) MRL/*lpr* mice (21, 22). We show here that estrogen deficiency caused a severe inflammatory arthritis in younger (<3-month-old) MRL/*lpr* mice, and these lesions were dramatically prevented by exogenous estrogen treatment. Although the mechanism in detail of estrogen activity still remains unclear, these findings suggest that estrogenic action has an important role during development of autoimmune arthritis in MRL/*lpr* mice. An estrogen deficiency by Ovx in murine RA model results in a significant increase of serum RF, anti-dsDNA Abs, and anti-CII Ab, and these changes were recovered by estrogen ad-

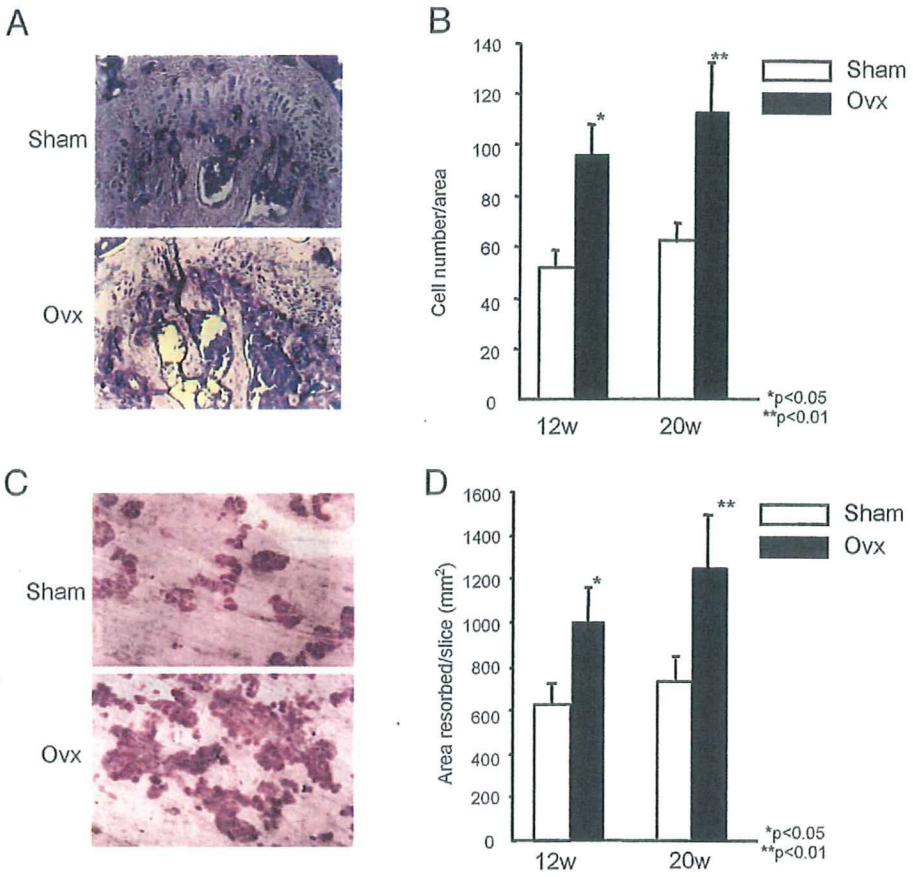

FIG. 5. Effect of the Ovx on OC formation and bone resorption assay. TRAP-positive OC-like cells were detected in the knee joints from both Ovx- and sham-MRL/*lpr* mice (A). A significantly increased number of OCs formed in the joints from Ovx-MRL/*lpr* mice at ages 12 (12w) and 20 wk (20w) was observed compared with those from sham-MRL/*lpr* mice (B) (*, $P < 0.05$ and **, $P < 0.01$, Student's t test). TRAP-positive multinucleated cells (more than three nuclei) from bone marrow cells were observed in both Ovx- and sham-MRL/*lpr* mice when cultured with dexamethasone (10^{-7} M) and $1\alpha,25\text{-}(OH)_2D_3$ (10^{-8} M) (C). A significantly large number of resorption pits was formed using the bone marrow cells from Ovx-MRL/*lpr* mice compared with those from sham-MRL/*lpr* mice (*, $P < 0.05$ and **, $P < 0.01$, Student's t test)(D).

ministration. A previous report has shown that treatment with low doses of β-estradiol exerts a suppressive effect on both development of collagen arthritis as well as T cell-dependent immune reactivity toward type II collagen (35). It was also reported that an estrogen deficiency stimulates B cell development (36) and autoantibody production (36–38), and its increase by an estrogen deficiency has been mediated by cytokines such as IL-6, IFN-γ, and TNF-α (39–41). A recent report has demonstrated that estrogen deficiency induces bone loss by increasing T cell proliferation through IFN-γ-induced class II transactivator (42).

Bone resorption is regulated by the immune system, in which T cell expression of RANKL, which is essential for osteoclastogenesis, may contribute to pathological conditions, such as RA (43). However, it remains unclear whether activated T cells maintain bone homeostasis by counterbalancing the action of RANKL. In this study, a significant increase of $CD4^+$ T cells bearing RANKL in the spleen and inguinal LN from Ovx-MRL/*lpr* mice was observed. Moreover, we detected an enhanced RANKL mRNA expression and $RANKL^+$ infiltrating cells in synovium from Ovx-MRL/*lpr* mice. In contrast, an impaired OPG concentration was found in synovial fluid, in addition to a decreased OPG mRNA in synovium of Ovx-MRL/*lpr* mice. Although molecular mechanisms demonstrating that the appearance of increased RANKL expression in T cells and synovium is related to the development of the autoimmune response are obscure, a role for RANKL in bone resorption in RA is suggested by the identification of RANKL mRNA and protein in cultured synovial fibroblasts from patients with RA and in $CD4^+$ and $CD8^+$ T cells in RA synovial tissues (10). Additional evidence that RANKL plays a critical role in the pathogenesis of bone destruction in inflammatory arthritis comes from studies in the rat adjuvant arthritis model (44, 45). Moreover, it has been recently demonstrated that up-regulation of RANKL on bone marrow cells is an important determinant of increased bone resorption induced by estrogen deficiency (46). Treatment with OPG also prevented OC accumulation, whereas destruction of bone in untreated arthritic animals was accompanied by the accumulation of large numbers of $TRAP^+$ OC-like cells (47). OPG treatment in an animal model of arthritis that is dependent on T cell activation has the potential for blocking not only the effects of RANKL on OC differentiation and activation but also the influence of RANKL on T cell-DC interactions (20).

OCs have a crucial role in the local bone destruction that occurs in association with chronic inflammatory diseases (48). Diseases such as RA have been associated with the accumulation of TNF-α and/or other proinflammatory cytokines such as IL-1 and IL-6, which likely mediate local bone destruction by stimulating OC activity (49). The results in the present study demonstrated an increased gene expression of cytokines including IL-1β, TNF-α, IL-6, IFN-γ, β-actin, and IRF-1 in the synovium from Ovx-MRL/*lpr* mice. In addition, an elevated gene expressions of MMP-3 and MMP-9 mRNA were observed in the synovium. Moreover, we found a significant increase in number of OCs, and bone resorption pits formed in Ovx-MRL/*lpr* mice. It has been shown that estro-

gen prevents bone loss through multiple effects on bone marrow and bone cells, which result in decreased OC formation (50), increased OC apoptosis (51), and decreased capacity of mature OCs to resorb bone (52). Because it was also demonstrated by direct evidence that treatment with estrogens suppressed RANKL-mediated OC formation (53), it is possible that their contribution to the increased osteoclastogenesis and the bone loss has been induced by estrogen deficiency.

In conclusion, we have demonstrated that activation of $CD4^+$ T cells bearing RANKL induced by an estrogen deficiency may play an important role on acceleration of autoimmune arthritis, and estrogenic action appears to influence joint destruction associated with RANKL-mediated osteoclastogenesis in a murine model for RA.

Acknowledgments

Received November 12, 2003. Accepted January 8, 2004.

Address all correspondence and requests for reprints to: Dr. Yoshio Hayashi, Department of Pathology, Tokushima University School of Dentistry, 3 Kuramotocho, Tokushima 770-8504, Japan. E-mail: hayashi@dent.tokushima-u.ac.jp.

This work was supported in part by a Grant-in-Aid for Scientific Research from the Ministry of Education, Science and Culture of Japan.

References

1. **Lahita RG, Bradlow L, Fishman J, HG Kunkel HG** 1982 Estrogen metabolism in systemic lupus erythematosus: patients and family members. Arthritis Rheum 25:843–846
2. **Zurier RB** 1987 Systemic lupus erythematosus. In: Lahita RG, ed. New York: Wiley Publishers; 541–554
3. **Daniels T, Whitcher JP** 1994 Association of patients of labial salivary gland inflammation with keratoconjunctivitis sicca. Analysis of 618 patients with suspected Sjögren's syndrome. Arthritis Rheum 37:869–877
4. **Davidson A, Diamond B** 2001 Autoimmune diseases. N Engl J Med 345:340–350
5. **Yamamura Y, Gupta R, Morita Y, He X, Pai R, Endres J, Freiberg A, Chung K, Fox DA** 2001 Effector function of resting T cells: activation of synovial fibroblasts. J Immunol 166:2270–2275
6. **Park CC, Morel JC, Amin MA, Connors MA, Harlow LA, Koch AE** 2001 Evidence of IL-18 as a novel angiogenic mediator. J Immunol 167:1644–1653
7. **van den Berg WB** 2001 Arguments for interleukin 1 as a target in chronic arthritis. Ann Rheum Dis 59:81–84
8. **Pap T, Shigeyama Y, Kuchen S, Fernihough JK, Simmen B, Gay RE, Billingham M, Gay S** 2000 Differential expression pattern of membrane-type matrix metalloproteinases in rheumatoid arthritis. Arthritis Rheum 43:1226–1232
9. **Takayanagi H, Iizuka H, Juji T, Nakagawa T, Yamamoto A, Miyazaki T, Koshihara Y, Oda H, Nakamura K, Tanaka S** 2000 Involvement of receptor activator of nuclear factor κB ligand/osteoclast differentiation factor in osteoclastogenesis from synoviocytes in rheumatoid arthritis. Arthritis Rheum 43:259–269
10. **Kotake S, Udagawa N, Hakoda M, Mogi M, Yano K, Tsuda E, Takahashi K, Furuya T, Ishiyama S, Kim KJ, Saito S, Nishikawa T, Takahashi N, Togari A, Tomatsu T, Suda T, Kamatani N** 2001 Activated human T cells directly induce osteoclastogenesis from human monocytes: possible role of T cells in bone destruction in rheumatoid arthritis patients. Arthritis Rheum 44:1003–1012
11. **Sabokbar A, Fujikawa Y, Neale S, Murray DW, Athanasou NA** 1997 Human arthroplasty derived macrophages differentiate into osteoclastic bone resorbing cells. Ann Rheum Dis 56:414–420
12. **Rothe L, Collin-Osdoby P, Chen Y, Sunyer T, Chaudhary L, Tsay A, Goldring S, Avioli L, Osdoby P** 1998 Human osteoclasts and osteoclast-like cells synthesize and release high basal and inflammatory stimulated levels of the potent chemokine interleukin-8. Endocrinology 139:4353–4363
13. **Gravallese EM, Manning C, Tsay A, Naito A, Pan C, Amento E, Goldring SR** 2000 Synovial tissue in rheumatoid arthritis is a source of osteoclast differentiation factor. Arthritis Rheum 43:250–258
14. **Wong B, Rho J, Arron J, Robinson E, Orlinick J, Chao M, Kalachikov S, Cayani E, Bartlett 3rd FS, Frankel WN, Lee SY, Choi Y** 1997 TRANCE is a novel ligand of the tumor necrosis factor receptor family that activates c-Jun N-terminal kinase in T cells. J Biol Chem 272:25190–25194
15. **Wong BR, Josien R, Choi Y** 1999 TRANCE is a TNF family member that regulates dendritic cell and osteoclast function. J Leukoc Biol 65:715–724
16. **Josien R, Wong BR, Li HL, Steinman RM, Choi Y** 1999 TRANCE, a TNF family member, is differentially expressed on T cell subsets and induces cytokine production in dendritic cells. J Immunol 162:2562–2568
17. **Anderson DM, Maraskovsky E, Billingsley WL, Dougall WC, Tometsko ME, Roux ER, Teepe MC, DuBose RF, Cosman D, Galibert L** 1997 A homologue of the TNF receptor and its ligand enhance T-cell growth and dendritic-cell function. Nature 390:175–179
18. **Josien R, Li HL, Ingulli E, Sarma S, Wong BR, Vologodskaia BM, Steinman RM, Choi Y** 2000 TRANCE, a tumor necrosis factor family member, enhances the longevity and adjuvant properties of dendritic cells in vivo. J Exp Med 191:495–502
19. **Bachmann MF, Wong BR, Josien R, Steinman RM, Oxenius A, Choi Y** 1999 TRANCE, a tumor necrosis factor family member critical for CD40 ligand-independent T helper cell activation. J Exp Med 189:1025–1031
20. **Wong BR, Josien R, Lee SY, Sauter B, Li HL, Steinman RM, Choi Y** 1997 TRANCE (tumor necrosis factor [TNF]-related activation-induced cytokine), a new TNF family member predominantly expressed in T cells, is a dendritic cell-specific survival factor. J Exp Med 186:2075–2080
21. **Cohen PL, Eisenberg RA** 1991 Lpr and gld: single gene models of systemic autoimmunity and lymphoproliferative disease. Annu Rev Immunol 9:243–269
22. **Theofilopuolos AN, Dixon FJ** 1985 Murine models of systemic lupus erythematosus. Adv Immunol 37:269–390
23. **Merino R, Iwamoto M, Fossati L, Izui S** 1993 Polyclonal B cell activation arises from different mechanisms in lupus-prone (NZBx NZW)F1 and MRL/MpJ-lpr/lpr mice. J Immunol 151:6509–6516
24. **Edwards 3rd CK, Zhou T, Zhang J, Baker TJ, De M, Long RE, Borcherding DR, Bowlin TL, Bluethmann H, Mountz JD** 1996 Inhibition of superantigen-induced proinflammatory cytokine production and inflammatory arthritis in MRL-lpr/lpr mice by a transcriptional inhibitor of TNF-α. J Immunol 157:1758–1772
25. **Feeney AJ, Lawson BR, Kono BDH, Theofilopoulos AN** 2001 Terminal deoxynucleotidyl transferase deficiency decreases autoimmune disease in MRL-Fas^{lpr} mice. J Immunol 167:3486–3493
26. **Fields ML, Sokol CL, Eaton-Bassiri A, Seo S, Madaio MP, Erikson J** 2001 Fas/fas ligand deficiency results in altered localization of anti-double-stranded DNA B cells and dendritic cells. J Immunol 167:2370–2378
27. **Kageyama Y, Koide Y, Yoshida A, Uchijima M, Arai T, Miyamoto S, Ozeki T, Hiyoshi M, Kushida K, Inoue T** 1998 Reduced susceptibility to collagen-induced arthritis in mice deficient in IFN-γ receptor. J Immunol 161:1542–1548
28. **Saegusa K, Ishimaru N, Yanagi K, Haneji N, Nishino M, Azuma M, Saito I, Hayashi Y** 2000 Autoantigen-specific $CD4^+CD28^{low}$ T cell subset prevents autoimmune exocrinopathy in murine Sjögren's syndrome. J Immunol 165:2251–2257
29. **Takahashi N, Yamana H, Yoshiki S, Roodman GD, Mundy GR, Jones SJ, Boyde A, Suda T** 1998 Osteoclast-like cell formation and its regulation by osteotropic hormones in mouse bone marrow cultures. Endocrinology 122:1373–1382
30. **Udagawa N, Takahashi N, Akatsu T, Tanaka H, Sasaki T, Nishihara T, Koga T, Martin TJ, Suda T** 1990 Origin of osteoclast: mature monocytes and macrophages are capable of differentiating into osteoclasts under a suitable microenvironment prepared by bone marrow-derived stromal cells. Proc Natl Acad Sci USA 87:7260–7264
31. **Choy EH, Panayi GS** 2001 Cytokine pathways and joint inflammation in rheumatoid arthritis. N Engl J Med 344:907–916
32. **Lahita RG** 1985 Sex steroids and the rheumatic diseases. Arthritis Rheum 28:121–126
33. **Bateman A, Singh A, Kral T** 1989 The immune-hypothalamic-pituitary-adrenal axis. Endocr Rev 10:92–112
34. **Grossman C** 1989 Possible underlying mechanisms of sexual dimorphism in the immune response, fact and hypothesis. J Steroid Biochem 34:241–251
35. **Holmdahl R, Jansson L, Meyerson B, Klareskog L** 1987 Oestrogen induced suppression of collagen arthritis: I. Long term oestradiol treatment of DBA/1 mice reduces severity and incidence of arthritis and decreases the anti-type II collagen immune response. Clin Exp Immunol 70:372–378
36. **Masuzawa T, Miura C, Onoe Y, Kusano K, Ohta H, Nozawa S, Suda T** 1994 Estrogen deficiency stimulates B lymphopoiesis in mouse bone marrow. J Clin Invest 94:1090–1097
37. **Verthelyi D, Ahmed SA** 1994 17β-estradiol, but not 5α-dihydrotestosterone, augments antibodies to double-stranded deoxyribonucleic acid in nonautoimmune C57BL/6 mice. Endocrinology 135:2615–2622
38. **Brick J, Walker S, Wise K** 1988 Hormone control to calf thymus nuclear extract (CTE) and DNA in MRL/lpr and MRL/+/+ mice. Clin Immunol Immunopathol 46:68–81
39. **Ralston SH** 1994 Analysis of gene expression in human bone biopsies by polymerase chain reaction: evidence for enhanced cytokine expression in postmenopausal osteoporosis. J Bone Miner Res 9:883–890
40. **Jilka RL, Hangoc G, Girasole G, Passeri G, Manolagas DC** 1992 Increased osteoclast development after estrogen loss: mediation by interleukin-6. Science 257:88–91